IEEE Access
Multidisciplinary ⋮ Rapid Review ⋮ Open Access Journal

Received 26 October 2023, accepted 21 November 2023, date of publication 30 November 2023,
date of current version 6 December 2023.

Digital Object Identifier 10.1109/ACCESS.2023.3337814

THEORY

Finite-Time Asynchronous Event-Triggered Control for Switched Nonlinear Cyber-Physical Systems With Quantization

ARUMUGAM ARUNKUMAR AND JENQ-LANG WU, (Member, IEEE)
Department of Electrical Engineering, National Taiwan Ocean University, Keelung 202301, Taiwan

Corresponding author: Jenq-Lang Wu (wujl@mail.ntou.edu.tw)

This work was supported by the National Science and Technology Council, Taiwan, under Grant 110-2811-E-019-505-MY2 and Grant 110-2221-E-019-073-MY2.

ABSTRACT This study examines the finite-time event-triggered control (ETC) problem for nonlinear switched cyber-physical systems (NSCPSs) by using an asynchronous switching strategy. An ETC scheme, along with a measurement size reduction technique, has been implemented to decrease network communication burden and redeem network resources. Data quantization is also another efficient method for reducing the amount of transmitted data via networks. Meanwhile, asynchronous phenomena among ETC instants are studied, which is much more realistic and difficult in the system under consideration. The prime intent of this research is to enhance the asynchronous event-triggered control (AETC) technique to guarantee the resulting closed-loop NSCPS is finite-time bounded (FTB) and prespecified mixed H_∞ and passive performance index γ in the finite-time horizon. A novel set of required conditions in the form of linear matrix inequalities (LMIs) is enhanced using the Lyapunov-Krasovskii functional (LKF) theory, ensuring that the FTB criterion is met. Furthermore, the gains are acquired by solving a group of LMIs. Ultimately, a numerical illustration is provided, showcasing the efficaciousness and practicality of the developed control strategy through a real-world application known as the vertical take-off and landing helicopter model (VTOLHM).

INDEX TERMS Nonlinear cyber-physical systems, asynchronous event-triggered scheme, quantization, finite-time control.

I. INTRODUCTION

Networked control systems (NCS) involving sensors, controllers, actuators, and networks are becoming increasingly important for modern society's structures, such as smart grids, intelligent housing, and public transit systems [1]. There is also no dispute that incorporating network infrastructure into control systems provides several benefits and conveniences owing to its high dependability, cheap cost, simplicity of installation, and maintenance across a wide range of practical applications [2]. Because of these advantages offered by NCSs, there is a sustained interest in investigating them, leading to numerous successful results [3], [4], [5], [6]. However, as a result of the insertion of the NCSs, various problematic phenomena like packet disorder, communication delays, data dropouts, and congestion occur [7]. Furthermore, switched systems, which are made up of a collection of subsystems linked by a switching mechanism that helped orchestrate their switching, are widely used in intelligent transportation systems, power electronics, robotic control systems, and other applications [8], [9], [10], [11], [12]. Different features of switched systems have been thoroughly investigated, but there has been limited research on switched systems that transmit data over communication networks. As such, it remains a highly significant problem to study switched systems with networked control, which are referred to as networked switched systems [13]. For example, the distributed H_∞ control design for switched linear NCS is analyzed in [14] subject to packet dropouts and quantization.

Communication channels are used to transfer signals in NCSs because sensor energy and communication network bandwidth are insufficient for many other communication

The associate editor coordinating the review of this manuscript and approving it for publication was Engang Tian.

© 2023 The Authors. This work is licensed under a Creative Commons Attribution-NonCommercial-NoDerivatives 4.0 License.
For more information, see https://creativecommons.org/licenses/by-nc-nd/4.0/

activities [15], [16], [17]. As a result, an alternative concept known as the ETC mechanism has emerged as a potential approach in NCSs, reducing the communication costs and computing burden while maintaining acceptable control performance [2]. In an ETC architecture, signals are broadcast only if the current signal meets the triggering level. Some important effects of the ETC method have been addressed due to high usage, enhancing communication bandwidth, and reducing energy resources [3], [4], [18], [19], [20]. By taking the advantage of ETC scheme, the authors in [17] studied the stability and stabilization problem for the networked systems subject to output feedback control design and cyber-attacks. In [15], an ETC strategy has been developed for the nonlinear networked system with limited network bandwidth and sampling-driven unmatched disturbance. An ETC strategy for switched NCSs has gotten a lot of attention recently, with some outstanding results reported in the literature [21], [22]. Recently, an ETC mechanism for networked switching systems across a finite horizon has been addressed in [13]. An observer-based ETC strategy for switched systems with output feedback control laws and mixed time-varying delays has also been investigated in [8]. In [21], an ETC mechanism is described for H_∞ switched networked systems with the assistance of the LKF theory.

Among the aforementioned results, a common assumption would be that the candidate controller usually switches synchronously with its subsystems. In reality, while employing the ETC technique in switched systems, the event may well not trigger at the time the system switches. As a result, when the system switches to a new mode, the prior controller remains active until the next event happens, resulting in asynchronism between subsystems and candidate controllers [23]. For instance, a new AETC mechanism is considered for T-S fuzzy switched systems in [4]. An asynchronous problem for fuzzy semi-Markov jump systems is discussed in [24] subject to ETC, reliable and extended passive control. In [18], an asynchronous switching problem is investigated for switched systems via an output ETC scheme. Recently, the issue of an event-triggered output regulation mechanism for switched NCSs with packet losses and transmission delays under asynchronous switching are exhibited in Li et al. [3].

Furthermore, from a pragmatic perspective, NCS security concerns have gotten a lot of attention in the control industry since a lot of data has to be transferred across a networked channel of communication which may be attacked by cyber-criminals. By exploiting vulnerable communication links, cyber-attackers attempt to send inaccurate control commands to control center operators. In recent years, various effective ways have been described for protecting against cyber-attacks and making perfect attacks impossible [25], [26], [27], [28], [29]. To mention a few, in [30], the authors developed a finite-time sliding-mode controller for a type of Markovian jump cyber-physical systems with randomly occurring injection attacks. The authors in [5] propose the stochastic cyber-attacks on hybrid-triggered guaranteed cost control for networked systems. According to [7], the authors have developed the issue of distributed ETC for NCSs by analyzing the implications of cyber-attacks. In [31], the cyber-attacks problem was investigated for multirate networked systems by using fading measurements and a round-robin approach. Very recently, in [32], cyber-attacks are taken into account while dealing with networked control systems using a hybrid-driven mechanism.

On the flip side, it's conceivable that the network has space restrictions on its packets. In the networked systems, persistent communication is an unavoidable phenomenon that results in high communication traffic and high energy consumption. Therefore, an energy-efficient measurement size reduction approach is developed, which effectively reduces transmission times. NCSs with measurement size reduction technique have received little attention in the literature. Only a few works have been explored based on this subject so far, for example, see [33]. For instance, in [34], the authors used the LKF technique to tackle the issue of an measurement size reduction approach for multiagent systems with the stochastic sampling and intermittent transmission. Zhang et al. [33] studied the problem of distributed filtering issues for non-fragile sensor networks with stochastic transmission and measurement size reduction techniques.

On the other hand, asymptotic/exponential stability of NCSs is well known to be characterized across an infinite time period, whereas finite-time stability or boundedness focuses on the important aspects of the given system in a finite-time period and does not exceed the specified threshold value [35], [36], [37], [38]. For practical control systems, finite-time stability is more conducive to achieving the quickest transient performance. As a result, a tremendous amount of research effort has been dedicated to finite-time stability, stabilization and boundedness issues, producing a significant quantity of results [11], [39], [40]. In the context of the finite-time control method, Ren et al. [9] developed the asynchronous switched networked systems. Additionally, the finite-time stabilization issues was explored in [41] for uncertain nonlinear systems with an ETC mechanism. It has been reported that numerous advanced techniques on a finite-time control of NCSs have already been published, but as far as we are aware, this has not yet been explored for the combination of H_∞ and passivity based ETC mechanism for NSCPSs with cyber-attacks and quantization over a finite-time span, especially for asynchronous cases.

Motivated by the above considerations, the present work investigates an AETC scheme that is able to achieve FTB strategies for NSCPSs with quantization and cyber-attacks. Based on a novel event-triggered communication scheme, an asynchronous controller is designed. Compared to existing works, the contributions of this paper are summarized as follows.

- In contrast to [7] and [17] an event-triggered-based asynchronous switching control approach is constructed to resolve the FTB problem.

- Based on the asynchronous approach [4], [20], [23], this is the first attempt to resolve the issue of uncertain NSCPSs susceptible to ETC scheme, cyber-attacks and quantization over a finite interval of time. Specifically, multiple switchings among two consecutive execution instants are considered, which leads to asynchronous phenomena and makes the system more practical and complicated.
- Compared with the work in [9], [13], and [18], our proposed results focus on the NSCPSs with quantization and cyber-attacks.
- In addition, to reduce energy consumption, a measurement size reduction approach is used. Furthermore, the randomly occurring cyber-attacks governed by a Bernoulli distributed variable are expressed as a nonlinear function fulfilling the restraining requirement.
- Utilizing Lyapunov stability theory, a novel set of criteria for achieving the required FTB criterion with prescribed finite time mixed H_∞ and passivity performance index has been constructed in the framework of LMI.

Eventually, a practical numerical example of a VTOLHM is presented to emphasize the effectiveness of the proposed control approach.

Notation: The notations used throughout this paper are standard which are unrevealed as follows: $\mathbb{R}^{n_x}$, $\mathbb{R}^{n_u}$, $\mathbb{R}^{n_w}$ and $\mathbb{R}^{n_z}$ represents the n_x, n_u, n_w and n_z-dimensional Euclidean space; $L_2[0,\infty)$ represents the space of square integrable functions over the interval $[0,\infty)$. $P > 0$ (≥ 0) means that P is real symmetric and positive definite (positive semi-definite). The superscripts "T" and "-1" stand for matrix transposition and matrix inverse, respectively. We use 0 and I to denote the zero and identity matrix with corresponding dimension. In symmetric block matrices or long matrix expressions, we use an asterisk ($*$) to represent a term that is induced by symmetry and diag{...} stands for a block-diagonal matrix.

II. PROBLEM DESCRIPTION

This article pays attention towards the finite-time AETC design problem for a class of NSCPSs as structured in Fig. 1. An ETC generator and energy limitations are used to conserve network resources. The event generators release the data, which is subsequently transferred to the controller through an unreliable network connection susceptible to cyber-attacks. Based on the above concern, the nonlinear switched system with disturbance signal is depicted in the following equation:

$$\begin{aligned}\dot{\mathcal{X}}(t) &= \hat{\mathcal{A}}_{\sigma(t)}(t)\mathcal{X}(t) + \mathcal{B}_{\sigma(t)}\mathcal{U}(t) + \hat{\mathcal{C}}_{\sigma(t)}(t)\mathcal{F}(\mathcal{X}(t)) \\ &\quad + \hat{\mathcal{D}}_{\sigma(t)}(t)\mathcal{W}(t), \\ \mathcal{Z}(t) &= \mathcal{E}_{\sigma(t)}\mathcal{X}(t) + \mathcal{H}_{\sigma(t)}\mathcal{W}(t) \end{aligned} \tag{1}$$

where $\mathcal{X}(t) \in \mathbb{R}^{n_x}$ is the state vector; $\mathcal{U}(t) \in \mathbb{R}^{n_u}$ is the control input; $\mathcal{W}(t) \in \mathbb{R}^{n_w}$ is said to be the disturbance input signal that corresponds to $L_2[0,\infty)$; $\mathcal{Z}(t) \in \mathbb{R}^{n_z}$ is the controller output; $\sigma(t)$ represents the switching signal that

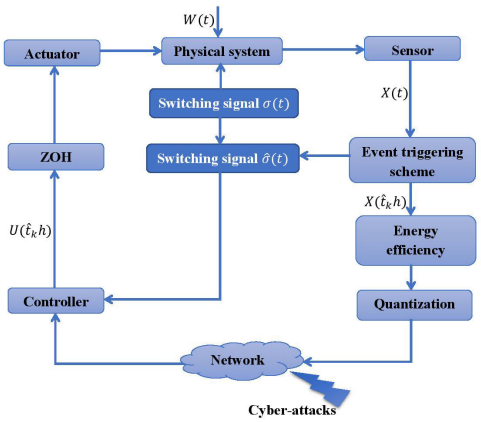

FIGURE 1. AETC framework of NSCPSs.

accepts values from a finite collection $\mathcal{I} = \{1, 2, \cdots, \mathcal{R}\}$; e.g. when $\sigma(t) = i \in \mathcal{I}$, it implies that the i^{th} subsystem has been enabled, where $\mathcal{R}$ denotes the number of subsystems; The matrices $\hat{\mathcal{A}}_i(t), \hat{\mathcal{C}}_i(t)$ and $\hat{\mathcal{D}}_i(t)$ are denoted as $\hat{\mathcal{A}}_i(t) = \mathcal{A}_i + \Delta\mathcal{A}_i(t)$; $\hat{\mathcal{C}}_i(t) = \mathcal{C}_i + \Delta\mathcal{C}_i(t)$; $\hat{\mathcal{D}}_i(t) = \mathcal{D}_i + \Delta\mathcal{D}_i(t)$; $\mathcal{A}_i, \mathcal{B}_i, \mathcal{C}_i, \mathcal{D}_i, \mathcal{E}_i$ and $\mathcal{H}_i$ are well-known constant matrices of suitable dimensions; Furthermore, the uncertainty in the parameters $\Delta\mathcal{A}_i(t), \Delta\mathcal{C}_i(t)$ and $\Delta\mathcal{D}_i(t)$ are satisfied as follows: $[\Delta\mathcal{A}_i(t)\ \Delta\mathcal{C}_i(t)\ \Delta\mathcal{D}_i(t)] = \mathcal{M}_{1i}\mathcal{F}_i(t)\,[\mathcal{N}_{1i}\,\mathcal{N}_{2i}\,\mathcal{N}_{3i}]$, where $\mathcal{M}_{1i}, \mathcal{N}_{1i}, \mathcal{N}_{2i}$ and $\mathcal{N}_{3i}$ are well-known constant matrices of required dimension, and $\mathcal{F}_i(t)$ seems to be an unknown time-varying function fulfilling $\mathcal{F}_i^T(t)\mathcal{F}_i(t) \leq I$, where I represents the identity matrix. Furthermore, $\mathcal{F}(\mathcal{X}(t)) = \left[\mathcal{F}_1(\mathcal{X}_1(t)), \mathcal{F}_2(\mathcal{X}_2(t)), \ldots, \mathcal{F}_n(\mathcal{X}_n(t))\right]^T$ is a nonlinear vector function which fulfills the global Lipschitz requirement $\|\mathcal{F}(t,\mathcal{X}) - \mathcal{F}(t,\mathcal{Y})\| \leq \beta_{\mathcal{F}}\|(\mathcal{X}-\mathcal{Y})\|, \forall \mathcal{X}, \mathcal{Y} \in \mathbb{R}^{n_f}$, where $\beta_{\mathcal{F}}$ is a positive scalar.

During control signal transmission, an event-based generator should be deployed to conserve communication resources [4], [42]. We develop an ETC method throughout the paper to establish the time sequence $\hat{t}_k h, k \in \mathbb{Z}^+$ with $\hat{t}_k h$ indicating the time instant when an event occurs and $h > 0$ is the sampling period. Besides that, the control input at the actuator has been produced by the zero-order-hold inside the holding interval $[\hat{t}_k h + \tau_{\hat{t}_k}, \hat{t}_{k+1}h + \tau_{\hat{t}_{k+1}})$, where $\tau_{\hat{t}_k}$ represents the communication delay at the release instant $\hat{t}_k h$. Furthermore, the ETC mechanism has been designed as follows:

$$\begin{aligned}\hat{t}_{k+1}h = \hat{t}_k h + \min_s \big\{ sh | e_{\hat{t}_k}^T(\hat{t}_k h + sh)\Phi_{1\hat{\sigma}(\hat{t}_k)} \\ e_{\hat{t}_k}(\hat{t}_k h + sh) > \varsigma_{\hat{\sigma}(\hat{t}_k)}\mathcal{X}^T(\hat{t}_k h)\Phi_{2\hat{\sigma}(\hat{t}_k)}\mathcal{X}(\hat{t}_k h)\big\} \end{aligned} \tag{2}$$

where $0 < \varsigma_{\hat{\sigma}(\hat{t}_k)} < 1$ are known parameters, $\Phi_{1\hat{\sigma}(\hat{t}_k)}$ and $\Phi_{2\hat{\sigma}(\hat{t}_k)}$ are the positive definite matrices to be generated, and $e_{\hat{t}_k}(\hat{t}_k h + sh)$ is perhaps the difference between the two states at the previous transmission instant and the subsequent sampling instant, i.e. $e_{\hat{t}_k}(i_k h) = \mathcal{X}(\hat{t}_k h) - \mathcal{X}(i_k h)$, where $i_k h = \hat{t}_k h + sh,\ s \in \mathbb{N}$.

Remark 1: We established a novel switching signal $\hat{\sigma}(t)$ in the ETC mechanism (2) which also accepts its values

in $\mathcal{R}$. At the execution instant $\hat{t}_k$, the values of $\hat{\sigma}(t)$ may well be updated, and $\hat{\sigma}(\hat{t}_k) = \sigma(\hat{t}_k)$. During the interval $[\hat{t}_k, \hat{t}_{k+1})$, it will remain unaltered. Let $\{t_s, s \in \mathbb{Z}^+\}$ indicate the switching sequence, where t_s represents the s^{th} switching instant satisfying $t_s < t_{s+1}$ and $t_0 = 0$. It should be remembered that the switching signal $\sigma(t)$ may only be modified at t_s. Finally, $\hat{\sigma}(t)$ may not be equal to $\sigma(t)$, at time instant t. For illustration, assuming $\hat{t}_k < t_s < \hat{t}_{k+1} < t_{s+1}$, then $\hat{\sigma}(t) \neq \sigma(t)$ for $t \in [t_s, \hat{t}_{k+1})$.

We generate the new state feedback controller based on the aforementioned trigger condition:

$$\overline{\mathcal{U}}(t) = \hat{\mathcal{K}}_{\hat{\sigma}(\hat{t}_k)} \mathcal{X}(\hat{t}_k h). \tag{3}$$

where, $\hat{\mathcal{K}}_{\hat{\sigma}(\hat{t}_k)}$ denotes the controller gain that must be determined for $\hat{\sigma}(\hat{t}_k) \in \mathcal{R}$.

As shown in Fig. 1, we designed an ETC framework. The employment of two switching signals $\sigma(t)$ and $\hat{\sigma}(t)$, which act in subsystems and controllers, respectively, distinguishes this control method from that in [42]. Subsystems and controllers switch synchronously, hence there is just one switching signal, according to [42]. It is evidently conservative since asynchronous switching is ignored because the switching feature with ETC transmission coexist. In our control scheme, the switching of subsystems is subject to $\sigma(t)$ while the switching of controllers is subject to $\hat{\sigma}(\hat{t}_k)$. As indicated in Remark 1, $\sigma(t)$ may not be equal to $\hat{\sigma}(t)$ at certain intervals. As a result, the modes of subsystems and controllers are mismatched at some of these intervals., i.e., the closed-loop system has asynchronous behavior.

It is worth noting that once the sample signal is released into the network at instant $\hat{t}_k h$, it will then be transmitted to the controller at instant $\hat{t}_k h + \tau_{\hat{t}_k}$, in which $\tau_{\hat{t}_k}$ is the communication delay induced by the network. Similarly to what is shown in [9], the interval represents $[\hat{t}_k h + \tau_{\hat{t}_k}, \hat{t}_{k+1} h + \tau_{\hat{t}_{k+1}})$, may be broken down into a number subintervals. Assume that there is a constant ν that fulfills $[\hat{t}_k h + \tau_{\hat{t}_k}, \hat{t}_{k+1} h + \tau_{\hat{t}_{k+1}}) = \bigcup_{s=0}^{\nu} \mathcal{T}_s$, where $\mathcal{T}_s = [\hat{t}_k h + sh + \tau_{\hat{t}_{k+s}}, \hat{t}_k h + sh + h + \tau_{\hat{t}_{k+s+1}}]$, $s = \{0, 1, \cdots, \nu\}$, $\nu = \hat{t}_{k+1} - \hat{t}_k - 1$. Define $\tau(t) = t - \hat{t}_k h - sh$, $0 \leq \tau_{\hat{t}_k} \leq \tau(t) \leq h + \tau_{\hat{t}_{k+s+1}} \leq \overline{\tau}$. It is possible that the network's packets have space limitations. Due to the power restriction, not all state components are permitted to be transferred. In this paper, only one element of signal component is picked for transmission and then encapsulated into a packet, as this is the most energy-efficient way [34]. Based on the work in [33], we define the structure of measurement selection scheme as

$$\varphi_{\rho(t)} \in \left[0, \cdots, \underbrace{1}_{n}, \cdots, 0 \right], \tag{4}$$

where $\rho(t) \in \Gamma = \{1, 2, \cdots, n\}$ is a time-varying signal that indicates which measurement element has been selected. For illustrate, while the first element is picked for transmission, we acquire $\rho(t) = 1$ and $\varphi_{\rho(t)} = \text{diag}\{1, 0, \cdots, 0\}$. Whenever the second element is picked for transmission, we get $\rho(t) = 2$ and $\varphi_{\rho(t)} = \text{diag}\{0, 1, \cdots, 0\}$. Depending on a similar concept, one might have more elements for transmission. Aside from that, the modified control signal can be formed as follows, based on the preceding discussion:

$$\begin{aligned} \hat{\mathcal{U}}(t) = \mathcal{K}_{\hat{\sigma}(\hat{t}_k)\rho(t)} \varphi_{\rho(t)} (\mathcal{X}(t - \tau(t)) + e_{\hat{t}_k}(t)), \\ t \in [\hat{t}_k h + \tau_{\hat{t}_k}, \hat{t}_{k+1} h + \tau_{\hat{t}_{k+1}}). \end{aligned} \tag{5}$$

Remark 2: In the aforementioned approach of reducing measurement size, we presume that only one element of the signal can be transmitted to the controller. The above can be expanded to other general cases. As we endeavor to reduce the energy consumption of the networked system, the less information we transmit, the less energy are consumed.

Basically, the control signals are often quantized due to high convention of digital signals. Thus, the data quantization $\breve{\mathcal{U}}(t)$ is examined in the following manner

$$\breve{\mathcal{U}}(t) = \mathcal{Q}(\hat{\mathcal{U}}(t)). \tag{6}$$

where $\mathcal{Q}(\cdot) = [\mathcal{Q}_1(\cdot), \mathcal{Q}_2(\cdot), \cdots, \mathcal{Q}_m(\cdot)]^T$ is a logarithmic quantizer and it is described by an odd function, i.e., $\mathcal{Q}_s(\upsilon) = -\mathcal{Q}_s(-\upsilon)$, $(s = 1, 2, \cdots, m)$. For each $\mathcal{Q}_s(u_s)$ it is defined as follows:

$$\mathcal{Q}_s(u_s^l) = \begin{cases} \eta_s^l, & if \ \dfrac{1}{1+\delta_{q_s}} \eta_s^l < u_s^l < \dfrac{1}{1-\delta_{q_s}} \eta_s^l, \\ 0, & if \ u_s = 0 \\ -\mathcal{Q}_s(-u_s), & if \ u_s < 0 \end{cases} \tag{7}$$

where $\delta_{q_s} = (1-\rho_s)/(1+\rho_s)$, $(0 < \rho_s < 1)$, the quantization density is ρ_s, and the set of quantization levels is defined by

$$\begin{aligned} \eta_s = \left\{ \pm \eta_s^l, \eta_s^l = \rho_s^l \eta_0^l, l = 0, \pm 1, \pm 2. \cdots \right\} \cup \{0\}, \\ 0 < \rho_s < 1, \ \ \eta_0^l > 0. \end{aligned} \tag{8}$$

Define $\Delta_q = \text{diag}\{\Delta_{q_1}, \Delta_{q_2}, \cdots, \Delta_{q_m}\}$, with $\Delta_{q_s} \in [-\delta_{q_s}, \delta_{q_s}]$, $s = 1, 2, \cdots, m$. The estimator's real input may thus be expressed as,

$$\breve{\mathcal{U}}(t) = \mathcal{Q}(\hat{\mathcal{U}}(t)) = (1 + \Delta_q) \hat{\mathcal{U}}(t) \tag{9}$$

In most cases, control data is transmitted via a communication network, which is vulnerable to malicious attacks from hackers. Further, cyber-attacks are carried out by destroying or modifying the controller inputs, and by exploiting the vulnerability of the communications networks, as well. As a consequence, the ETC mechanism with cyber-attacks looks like this:

$$\begin{aligned} \mathcal{U}(t) = \widetilde{\mathcal{U}}(t) = \beta(t) \mathcal{K}_{\hat{\sigma}(\hat{t}_k)\rho(t)} \varphi_{\rho(t)} (1 + \Delta_q) (\mathcal{X}(t - \tau(t)) \\ + e_{\hat{t}_k}(t)) + (1 - \beta(t)) \mathcal{K}_{\hat{\sigma}(\hat{t}_k)\rho(t)} \varphi_{\rho(t)} \\ \times (1 + \Delta_q) \mathcal{G}(\mathcal{X}(t - d(t))). \end{aligned} \tag{10}$$

where, $\beta(t) \in \mathcal{R}$ is a stochastic variable representing the Bernoullis distributed white series with $\text{Prob}\{\beta(t) = 1\} = \overline{\beta}$, $\text{Prob}\{\beta(t) = 0\} = 1 - \overline{\beta}$; $\mathcal{G}(\mathcal{X}(t))$ illustrates the function of cyber-attack; $d(t)$ indicates the time-varying delay of a

cyber-attack that fulfills $0 \leq d(t) \leq \overline{d}$, where $\overline{d}$ is a positive constant.

In order to keep things simple, this paper assumes $\hat{\sigma}(\hat{t}_k) = j \in \mathcal{R}$ and $\rho(t) = a$. Then the closed-loop NSCPS (1) along with (3), (5), (9), (10) can be revealed in the following ways:

$$\begin{aligned}&\dot{\mathcal{X}}(t)\\&= \hat{\mathcal{A}}_i(t)\mathcal{X}(t) + \mathcal{B}_i\mathcal{K}_{ja}\varphi_a(1+\Delta_q)\big(e_{\hat{t}_k}(t) + \overline{\beta}(\mathcal{X}(t-\tau(t)))\\&\quad + (1-\overline{\beta})\mathcal{G}(\mathcal{X}(t-d(t)))\big) + (\beta(t)-\overline{\beta})(\mathcal{X}(t-\tau(t))\\&\quad + e_{\hat{t}_k}(t) - \mathcal{G}(\mathcal{X}(t-d(t)))) + \hat{\mathcal{C}}_i(t)\mathcal{F}(\mathcal{X}(t)) + \hat{\mathcal{D}}_i(t)\mathcal{W}(t).\end{aligned} \tag{11}$$

Besides that, the assumptions and definitions in the forthcoming section are more crucial for substantiating the needed results.

Assumption 1: The nonlinear functions $\mathcal{G}(\mathcal{X}(t))$ be the randomly occurring cyber-attack satisfy $\|\mathcal{G}(\mathcal{X}(t))\|_2 \leq \beta_{\mathcal{G}}\|\mathcal{X}(t)\|_2$, where $\beta_{\mathcal{G}}$ represent a positive scalar.

Assumption 2: For the time-varying exterior disturbance input $\mathcal{W}(t)$, a given positive parameter β, and achieves $\int_0^{\mathscr{T}_f}\mathcal{W}^T(t)\mathcal{W}(t)dt \leq \beta$, where $\beta \geq 0$ and $[0, \mathscr{T}_f]$ is a fixed finite-time period.

Definition 1: [18] For any $\mathscr{T}_f \geq t \geq 0$, let $N_\sigma(t, \mathscr{T}_f)$ indicate the switching number of $\sigma(t)$ over $(t, \mathscr{T}_f)$. If $N_\sigma(t, \mathscr{T}_f) \leq N_0 + \frac{\mathscr{T}_f - t}{\tau_a}$ holds for an integer $N_0 \geq 0$ and $\tau_a > 0$, then τ_a is referred to as average dwell time.

Definition 2: [9] In the presence of positive constants $\mathscr{C}_1, \mathscr{C}_2$ and $\mathscr{T}_f$ with $\mathscr{C}_1 < \mathscr{C}_2$, a positive definite matrix $\mathscr{L}$ and an external disturbance $\mathcal{W}(t)$ satisfying Assumption 2, the closed-loop NSCPS (11) is said to be FTB with respect to $(\mathscr{C}_1, \mathscr{C}_2, \mathscr{T}_f, \beta, \mathscr{L})$ if for any $t \in [0, \mathscr{T}_f]$

$$\begin{aligned}&\mathbb{E}\left\{\max\left\{\sup_{-\tau\leq t_0\leq 0}\mathcal{X}^T(t_0)\mathscr{L}\mathcal{X}(t_0), \sup_{-\tau\leq t_0\leq 0}\dot{\mathcal{X}}^T(t_0)\mathscr{L}\dot{\mathcal{X}}(t_0)\right\}\right\}\\&\quad\leq \mathscr{C}_1 \Rightarrow \mathbb{E}\left\{\mathcal{X}^T(t)\mathscr{L}\mathcal{X}(t)\right\} < \mathscr{C}_2, \quad t \in [0, \mathscr{T}_f],\end{aligned}$$

We propose an AETC issue for NSCPS (11) in the perspective of quantization across a finite-time interval in this investigation. In particular, we will construct the proposed controller in such a manner that the closed-loop NSCPS (11) is robustly FTB with respect to $(\mathscr{C}_1, \mathscr{C}_2, \mathscr{T}_f, \beta, \mathscr{L})$ and fulfills specified performance measure, that seems to be, robustly finite-time mixed H_∞ and passive performance index, the following inequality holds:

$$\begin{aligned}&\int_0^{\mathscr{T}_f}\mathbb{E}\left\{\left(\gamma^{-1}\theta\mathcal{Z}^T(t)\mathcal{Z}(t) - 2(1-\theta)\mathcal{Z}^T(t)\mathcal{W}(t)\right)dt\right\}\\&\quad\leq \gamma\int_0^{\mathscr{T}_f}\mathbb{E}\left\{\mathcal{W}^T(t)\mathcal{W}(t)dt\right\}\end{aligned} \tag{12}$$

where $\theta \in [0, 1]$ is perhaps a weighting parameter that specifies the trade-off between H_∞ and passivity performances.

III. MAIN RESULTS

The issue of AETC for NSCPS (11) based on FTB and average dwell time technique with quantization design is concerned in this section. More accurately, we develop a new set of sufficient criterion for the existence of AETC design that can be assessed in terms of LMIs, which makes the NSCPS (11) is FTB, based on the adequate LKF and the mixed H_∞ and passivity performance.

A. FTB AND AVERAGE DWELL-TIME ANALYSIS

In this part, we construct sufficient conditions for the closed-loop NSCPS (11) robustly FTB, as well as an AETC scheme with cyber-attck.

Theorem 1: For given communication channel parameter $0 \leq \overline{\beta} \leq 1$, trigger parameter ς_j, nonnegative real scalars $\overline{\tau}, \overline{d}$, the other parameters $\alpha, \mu, \rho, \mathscr{C}_1, \mathscr{C}_2, \mathscr{T}_f, \beta$, the controller gain matrices $\mathcal{K}_{ja}$, then the NSCPS (11) with AETC sampling technique and cyber-attacks is robustly FTB with respect to $(\mathscr{C}_1, \mathscr{C}_2, \mathscr{T}_f, \beta, \mathscr{L})$ if there exist symmetric matrices $\mathcal{P}_{ia}, \mathcal{Q}_{1ia}, \mathcal{Q}_{2ia}, \mathcal{R}_{1ia}, \mathcal{R}_{2ia}, \mathcal{T}_{ia}, \Phi_{1j}, \Phi_{2j}$, appropriate dimensioned matrices $\mathcal{M}_{lia}(l = 1, 2)$ and scalars $\beta_{\mathcal{F}}, \beta_{\mathcal{G}}, \epsilon_1$ such that the following LMIs applicable for all $i, j \in \mathcal{R}$ and $a \in \Gamma$:

$$\Psi = \begin{bmatrix}\Psi_{\nu_1} & * & *\\ \Psi_{\nu_2} & -\wp_1 & *\\ \Psi_{\nu_3} & 0 & -\wp_2\end{bmatrix} < 0 \tag{13}$$

$$\begin{aligned}&\mathcal{P}_{ia} \leq \mu\mathcal{P}_{ja}, \mathcal{Q}_{1ia} \leq \mu\mathcal{Q}_{1ja}, \mathcal{Q}_{2ia} \leq \mu\mathcal{Q}_{2ja},\\&\mathcal{R}_{1ia} \leq \mu\mathcal{R}_{1ja}, \mathcal{R}_{2ia} \leq \mu\mathcal{R}_{2ja},\end{aligned} \tag{14}$$

$$\mathscr{W}_1\mathscr{C}_1 + \lambda_{12}\beta < \lambda_1\mathscr{C}_2\mu^{N_0}e^{-\alpha\mathscr{T}_f} \tag{15}$$

$$\begin{bmatrix}\mathcal{R}_{lia} & *\\ \mathcal{M}_{lia} & \mathcal{R}_{lia}\end{bmatrix} > 0, \quad (l = 1, 2) \tag{16}$$

and also any switching signal $\sigma(t)$ with the average dwell time fulfilling

$$\tau_a > \tau_a^* = \frac{\mathscr{T}_f \ln\mu}{\mathscr{T}_f - \mathscr{A}} \tag{17}$$

where

$$\Psi_{\nu_1} = \begin{bmatrix}\Psi_{1\nu} & * & *\\ \Psi_{2\nu} & \Psi_{3\nu} & *\\ \Psi_{4\nu} & 0 & \Psi_{5\nu}\end{bmatrix},$$

$$\Psi_{\nu_2} = \begin{bmatrix}\Psi_{\nu_{21}}^T & \Psi_{\nu_{22}}^T & \Psi_{\nu_{23}}^T & \Psi_{\nu_{24}}^T & \Psi_{\nu_{25}}^T & \Psi_{\nu_{26}}^T & \Psi_{\nu_{27}}^T\end{bmatrix}^T,$$

$$\Psi_{\nu_3} = \begin{bmatrix}\Psi_{\nu_{31}}^T & \Psi_{\nu_{32}}^T & \Psi_{\nu_{33}}^T & \Psi_{\nu_{34}}^T\end{bmatrix}^T,$$

$$\wp_1 = \mathrm{diag}\{0, \mathcal{R}_{1ia}^{-1}, \mathcal{R}_{2ia}^{-1}, \mathcal{R}_{1ia}^{-1}, \mathcal{R}_{2ia}^{-1}, \beta_{\mathcal{F}}, \beta_{\mathcal{G}}\},$$

$$\wp_2 = \mathrm{diag}\{\epsilon_{1i}, \epsilon_{1i}, \epsilon_{1i}, \epsilon_{1i}\},$$

$$\Psi_{1\nu} = \begin{bmatrix}\Psi_{1\nu 11} & * & *\\ \Psi_{1\nu 21} & \Psi_{1\nu 22} & *\\ \Psi_{1\nu 31} & \Psi_{1\nu 32} & \Psi_{1\nu 33}\end{bmatrix},$$

$$\Psi_{2\nu} = \begin{bmatrix}e^{-\alpha\overline{d}}(\mathcal{R}_{2ia} - \mathcal{M}_{2ia}) & 0 & 0\\ e^{-\alpha\overline{d}}\mathcal{M}_{2ia} & 0 & 0\\ 2\mathcal{C}_i^T\mathcal{P}_{ia}^T & 0 & 0\end{bmatrix},$$

$$\Psi_{3\nu} = \begin{bmatrix}\Psi_{3\nu 11} & * & *\\ \Psi_{3\nu 21} & \Psi_{3\nu 22} & *\\ 0 & 0 & -\beta_{\mathcal{F}}\end{bmatrix},$$

$$\Psi_{4\nu}=\begin{bmatrix}2(1-\overline{\beta})(1+\Delta_q)\varphi_a^T\mathcal{K}_{ja}^T\mathcal{B}_i^T\mathcal{P}_{ia}^T & 0 & 0\\ 2\overline{\beta}(1+\Delta_q)\varphi_a^T\mathcal{K}_{ja}^T\mathcal{B}_i^T\mathcal{P}_{ia}^T & 0 & 0\\ 2\mathcal{D}_i^T\mathcal{P}_{ia}^T & 0 & 0\end{bmatrix},$$

$$\Psi_{1\nu11}=2\mathcal{P}_{ia}\mathcal{A}_i+\mathcal{Q}_{lia}-e^{-\alpha\overline{\tau}}\mathcal{R}_{1ia}-e^{-\alpha\overline{d}}\mathcal{R}_{2ia}+\alpha\mathcal{P}_{ia},$$
$$\Psi_{1\nu21}=2\overline{\beta}(1+\Delta_q)\varphi_a^T\mathcal{K}_{ja}^T\mathcal{B}_i^T\mathcal{P}_{ia}^T+e^{-\alpha\overline{\tau}}(\mathcal{R}_{1ia}-\mathcal{M}_{1ia}),$$
$$\Psi_{1\nu22}=e^{-\alpha\overline{\tau}}(-2\mathcal{R}_{1ia}+\mathcal{M}_{1ia}^T+\mathcal{M}_{1ia})+\varsigma_j\Phi_{2j},$$
$$\Psi_{1\nu31}=e^{-\alpha\overline{\tau}}\mathcal{M}_{1ia},\ \Psi_{3\nu11}=e^{-\alpha\overline{d}}(-2\mathcal{R}_{2ia}+\mathcal{M}_{2ia}^T+\mathcal{M}_{2ia}),$$
$$\Psi_{1\nu33}=-e^{-\alpha\overline{\tau}}(\mathcal{Q}_{1ia}+\mathcal{R}_{1ia}),\ \Psi_{1\nu32}=e^{-\alpha\overline{\tau}}(\mathcal{R}_{1ia}-\mathcal{M}_{1ia}),$$
$$\Psi_{3\nu21}=e^{-\alpha\overline{d}}(\mathcal{R}_{2ia}-\mathcal{M}_{2ia}),\ \Psi_{3\nu22}=-e^{-\alpha\overline{d}}(\mathcal{Q}_{2ia}-\mathcal{R}_{2ia}),$$
$$\Psi_{5\nu}=\mathrm{diag}\{-\beta_{\mathcal{G}},-\Phi_{1j},-\mathcal{T}_{ia}\},$$
$$\Psi_{\nu_{22}}=\overline{\tau}\big[\mathcal{A}_i\ \ \overline{\beta}\mathcal{B}_i\mathcal{K}_{ja}\varphi_a(1+\Delta_q)\ 0_{3n}\ \ \mathcal{C}_i\ \ (1-\overline{\beta})\mathcal{B}_i\mathcal{K}_{ja}\varphi_a(1+\Delta_q)\ \ \overline{\beta}\mathcal{B}_i\mathcal{K}_{ja}\varphi_a(1+\Delta_q)\ \ \mathcal{D}_i\big],$$
$$\Psi_{\nu_{23}}=\overline{d}\big[\mathcal{A}_i\ \ \overline{\beta}\mathcal{B}_i\mathcal{K}_{ja}\varphi_a(1+\Delta_q)\ \ 0_{3n}\ \ \mathcal{C}_i\ \ (1-\overline{\beta})\mathcal{B}_i\mathcal{K}_{ja}\varphi_a(1+\Delta_q)\ \ \overline{\beta}\mathcal{B}_i\mathcal{K}_{ja}\varphi_a(1+\Delta_q)\ \ \mathcal{D}_i\big],$$
$$\Psi_{\nu_{24}}=\overline{\tau}\beta_1(1+\Delta_q)\times\big[0\ \ \mathcal{B}_i\mathcal{K}_{ja}\varphi_a\ \ 0_{4n}\ \ -\mathcal{B}_i\mathcal{K}_{ja}\varphi_a\ \ \mathcal{B}_i\mathcal{K}_{ja}\varphi_a\ \ 0\big],$$
$$\Psi_{\nu_{25}}=\overline{d}\beta_1(1+\Delta_q)\times\big[0\ \ \mathcal{B}_i\mathcal{K}_{ja}\varphi_a\ \ 0_{4n}\ \ -\mathcal{B}_i\mathcal{K}_{ja}\varphi_a\ \ \mathcal{B}_i\mathcal{K}_{ja}\varphi_a\ \ 0\big],$$
$$\Psi_{\nu_{26}}=\big[\mathscr{F}\quad 0_{8n}\big],\ \Psi_{\nu_{27}}=\big[0\quad\mathscr{G}\quad 0_{7n}\big],$$
$$\Psi_{\nu_{31}}=\big[0_{10n}\quad\overline{\tau}\mathcal{M}_{ia}^T\quad 0_{5n}\big],\ \Psi_{\nu_{33}}=\big[\mathcal{M}_{ia}^T\quad 0_{15n}\big],$$
$$\Psi_{\nu_{32}}=\Psi_{\nu_{34}}=\big[\epsilon_{1i}\mathcal{N}_{1i}\quad 0_{4n}\quad\epsilon_{1i}\mathcal{N}_{2i}\quad 0\quad\epsilon_{1i}\mathcal{N}_{3i}\quad 0_{8n}\big],$$
$$\mathscr{W}_1=\lambda_2+\overline{\tau}e^{-\alpha\overline{\tau}}\lambda_3+\overline{d}e^{-\alpha\overline{d}}\lambda_4+\frac{\overline{\tau}^2}{2}e^{-\alpha\overline{\tau}}\lambda_5+\frac{\overline{d}^2}{2}e^{-\alpha\overline{d}}\lambda_6,$$
$$\mathscr{F}_{\mathscr{A}}=\ln(\lambda_1\mathscr{C}_2)-\alpha\mathscr{T}_f-N_0\ln\mu-\ln(\mathscr{W}_1\mathscr{C}_1+\lambda_{12}\beta)$$

and other parameters are zero.

Proof: To achieve the desired result, the LKF for the closed-loop NSCPS (11) is constructed in the following form:

$$\begin{aligned}\mathcal{V}_i(\mathcal{X}(t))=&\mathcal{X}^T(t)\mathcal{P}_{ia}\mathcal{X}(t)+\int_{t-\overline{\tau}}^{t}e^{\alpha(s-t)}\mathcal{X}^T(s)\mathcal{Q}_{1ia}\mathcal{X}(s)ds\\&+\int_{t-\overline{d}}^{t}e^{\alpha(s-t)}\mathcal{X}^T(s)\mathcal{Q}_{2ia}\mathcal{X}(s)ds\\&+\overline{\tau}\int_{t-\overline{\tau}}^{t}\int_{\theta}^{t}e^{\alpha(s-t)}\dot{\mathcal{X}}^T(s)\mathcal{R}_{1ia}\dot{\mathcal{X}}(s)dsd\theta\\&+\overline{d}\int_{t-\overline{d}}^{t}\int_{\theta}^{t}e^{\alpha(s-t)}\dot{\mathcal{X}}^T(s)\mathcal{R}_{2ia}\dot{\mathcal{X}}(s)dsd\theta.\end{aligned}\tag{18}$$

By calculating the derivatives of $V_i(\mathcal{X}(t))$ and then taking into account both sides' mathematical expectations, we may arrive at

$$\begin{aligned}&\mathbb{E}\{\dot{\mathcal{V}}_i(\mathcal{X}(t))+\alpha\mathcal{V}_i(\mathcal{X}(t))\}\\&=2\mathcal{X}^T(t)\mathcal{P}_{ia}\dot{\mathcal{X}}(t)+\mathcal{X}^T(t)\\&(\alpha\mathcal{P}_{ia}+\mathcal{Q}_{1ia}+\mathcal{Q}_{2ia})\mathcal{X}(t)-e^{-\alpha\overline{\tau}}\mathcal{X}^T(t-\overline{\tau})\mathcal{Q}_{1ia}\mathcal{X}(t-\overline{\tau})\\&-e^{-\alpha\overline{d}}\mathcal{X}^T(t-\overline{d})\mathcal{Q}_{2ia}\mathcal{X}(t-\overline{d})+\overline{\tau}^2\mathbb{E}\{\dot{\mathcal{X}}^T(t)\mathscr{R}\dot{\mathcal{X}}(t)\}\\&-\overline{\tau}e^{-\alpha\overline{\tau}}\int_{t-\overline{\tau}}^{t}\dot{\mathcal{X}}^T(s)\mathcal{R}_{1ia}\dot{\mathcal{X}}(s)ds\\&-\overline{d}e^{-\alpha\overline{d}}\int_{t-\overline{d}}^{t}\dot{\mathcal{X}}^T(s)\mathcal{R}_{2ia}\dot{\mathcal{X}}(s)ds.\end{aligned}\tag{19}$$

where, $\mathscr{R}=\overline{\tau}^2\mathcal{R}_{1ia}+\overline{d}^2\mathcal{R}_{2ia}$. Furthermore, it should have been mentioned that

$$\mathbb{E}\{\dot{\mathcal{X}}^T(t)\mathscr{R}\dot{\mathcal{X}}(t)\}=\aleph_1^T\mathscr{R}\aleph_1+\beta_1\aleph_2^T\mathscr{R}\aleph_2\tag{20}$$

in which

$$\begin{aligned}\aleph_1=&\hat{\mathcal{A}}_i(t)\mathcal{X}(t)+\mathcal{B}_i\mathcal{K}_{ja}\varphi_a(1+\Delta_q)\big(\overline{\beta}(\mathcal{X}(t-\tau(t))+e_{\hat{\imath}_k}(t))\\&+(1-\overline{\beta})\mathcal{G}(\mathcal{X}(t-d(t)))\big)+\hat{\mathcal{C}}_i(t)\mathcal{F}(\mathcal{X}(t))+\hat{\mathcal{D}}_i(t)\mathcal{W}(t),\\\aleph_2=&\mathcal{B}_i\mathcal{K}_{ja}\varphi_a(1+\Delta_q)\big(\mathcal{X}(t-\tau(t))+e_{\hat{\imath}_k}(t)\\&-\mathcal{G}(\mathcal{X}(t-d(t)))\big).\end{aligned}$$

According to Lemma 1 in [26] for matrices $\mathcal{M}_{lia}(l=1,2)$, the integral terms in (19) can be expressed as

$$-\overline{\tau}e^{-\alpha\overline{\tau}}\int_{t-\overline{\tau}}^{t}\dot{\mathcal{X}}^T(s)\mathcal{R}_{1ia}\dot{\mathcal{X}}(s)ds\le e^{-\alpha\overline{\tau}}\xi_1^T(t)\Gamma_1\xi_1(t),\tag{21}$$
$$-\overline{d}e^{-\alpha\overline{d}}\int_{t-\overline{d}}^{t}\dot{\mathcal{X}}^T(s)\mathcal{R}_{2ia}\dot{\mathcal{X}}(s)ds\le e^{-\alpha\overline{d}}\xi_2^T(t)\Gamma_2\xi_2(t).\tag{22}$$

where,

$$\xi_1(t)=\big[\mathcal{X}^T(t)\quad\mathcal{X}^T(t-\tau(t))\quad\mathcal{X}^T(t-\overline{\tau})\big]^T,$$
$$\xi_2(t)=\big[\mathcal{X}^T(t)\quad\mathcal{X}^T(t-d(t))\quad\mathcal{X}^T(t-\overline{d})\big]^T,$$
$$\Gamma_l=\begin{bmatrix}-\mathcal{R}_{lia} & * & *\\ \mathcal{R}_{lia}-\mathcal{M}_{lia} & \hat{\Gamma}_l & *\\ \mathcal{M}_{lia} & \mathcal{R}_{lia}-\mathcal{M}_{lia} & -\mathcal{R}_{lia}\end{bmatrix},$$
$$\hat{\Gamma}_l=-2\mathcal{R}_{lia}+\mathcal{M}_{lia}+\mathcal{M}_{lia}^T,\ (l=1,2).$$

Furthermore, from Assumption 1, we attain that

$$\begin{aligned}&\beta_{\mathcal{G}}^{-1}\mathcal{X}^T(t-d(t))\mathscr{G}^T\mathscr{G}\mathcal{X}(t-d(t))\\&\quad-\beta_{\mathcal{G}}\mathcal{G}^T(\mathcal{X}(t-d(t)))\mathcal{G}(\mathcal{X}(t-d(t)))>0,\end{aligned}\tag{23}$$
$$\beta_{\mathcal{F}}^{-1}\mathcal{X}^T(t)\mathscr{F}^T\mathscr{F}\mathcal{X}(t)-\beta_{\mathcal{F}}\mathcal{F}^T(\mathcal{X}(t))\mathcal{F}(\mathcal{X}(t))\quad>0.\tag{24}$$

By unifying (18)-(24) with (2) and then utilizing the Schur complement Lemma, it is simple to derive that

$$\begin{aligned}&\mathbb{E}\{\dot{\mathcal{V}}_i(\mathcal{X}(t))+\alpha V_i(\mathcal{X}(t))-\mathcal{W}^T(t)\mathcal{T}_{ia}\mathcal{W}(t)\\&\quad-e_{\hat{\imath}_k}^T(t)\Phi_{1j}e_{\hat{\imath}_k}(t)+\varsigma_j\mathcal{X}^T(t-\tau(t))\Phi_{2j}\mathcal{X}(t-\tau(t))\}\\&=\Xi^T(t)\Psi\Xi(t),\end{aligned}\tag{25}$$

where $\Xi^T(t)=\Big[\xi_1^T(t)\ \ \mathcal{X}^T(t-d(t))\ \ \mathcal{X}^T(t-\overline{d})\ \mathcal{F}^T(\mathcal{X}(t))\ \mathcal{G}^T(\mathcal{X}(t-d(t)))\ e_{\hat{\imath}_k}^T(t)\ \mathcal{W}^T(t)\Big]$ and the element of Ψ are detailed in (13).

According to the approach in [39], the inequality (25) may be rephrased in the following way:

$$\mathbb{E}\{\dot{\mathcal{V}}_i(\mathcal{X}(t))+\alpha V_i(\mathcal{X}(t))\}-\mathcal{W}^T(t)\mathcal{T}_{ia}\mathcal{W}(t)<0.\tag{26}$$

Furthermore, integrating (26) with t_k to t results in

$$\mathbb{E}\{\mathcal{V}_i(\mathcal{X}(t))\}<e^{\alpha(t-t_k)}\mathbb{E}\{\mathcal{V}_i(\mathcal{X}(t_k))\}$$

$$+\int_{t_k}^{t} e^{\alpha(t-s)}\mathcal{W}^T(s)\mathcal{T}_{ia}\mathcal{W}(s)ds. \tag{27}$$

Make the assumption that, as the switching instants t_k, the NSCPS (11) switches from j^{th} subsystem to i^{th} subsystem; i. e., $\sigma(t_k^-) = j,\ \sigma(t_k^+) = \sigma(t_k) = i$ and employing (14), we acquire

$$\begin{aligned}
\mathbb{E}\{\mathcal{V}_i(\mathcal{X}(t))\} &< e^{\alpha(t-t_k)}\mu\mathcal{V}_i(\mathcal{X}(t_k^-))\\
&\quad+\int_{t_k}^{t} e^{\alpha(t-s)}\mathcal{W}^T(s)\mathcal{T}_{ia}\mathcal{W}(s)ds,\\
&< e^{\alpha(t-t_k)}\mu\big[e^{\alpha(t_k-t_{k-1})}\mathcal{V}_i(\mathcal{X}(t_{k-1}))\\
&\quad+\int_{t_{k-1}}^{t_k} e^{\alpha(t_k-s)}\mathcal{W}^T(s)\mathcal{T}_{ia}\mathcal{W}(s)ds\big]\\
&\quad+\int_{t_k}^{t} e^{\alpha(t-s)}\mathcal{W}^T(s)\mathcal{T}_{ia}\mathcal{W}(s)ds,\\
&= e^{\alpha(t-t_{k-1})}\mu\mathcal{V}_i(\mathcal{X}(t_{k-1}))\\
&\quad+\mu\int_{t_{k-1}}^{t_k} e^{\alpha(t-s)}\mathcal{W}^T(s)\mathcal{T}_{ia}\mathcal{W}(s)ds\\
&\quad+\int_{t_k}^{t} e^{\alpha(t-s)}\mathcal{W}^T(s)\mathcal{T}_{ia}\mathcal{W}(s)ds<\cdots,\\
&< e^{\alpha(t-0)}\mu^{N_\sigma(0,t)}\mathcal{V}_i(\mathcal{X}(0))\\
&\quad+\mu^{N_\sigma(0,t)}\int_{0}^{t_1} e^{\alpha(t-s)}\mathcal{W}^T(s)\mathcal{T}_{ia}\mathcal{W}(s)ds\\
&\quad+\mu^{N_\sigma(t_1,t)}\int_{t_1}^{t_2} e^{\alpha(t-s)}\mathcal{W}^T(s)\mathcal{T}_{ia}\mathcal{W}(s)ds\\
&\quad+\cdots+\mu\int_{t_{k-1}}^{t} e^{\alpha(t-s)}\mathcal{W}^T(s)\mathcal{T}_{ia}\mathcal{W}(s)ds\\
&\quad+\int_{t_k}^{t} e^{\alpha(t-s)}\mathcal{W}^T(s)\mathcal{T}_{ia}\mathcal{W}(s)ds,\\
&\le e^{\alpha\mathscr{T}_f}\mu^{N_\sigma(0,\mathscr{T}_f)}\big(\mathbb{E}\{\mathcal{V}_i(\mathcal{X}(0))\}\\
&\quad+\int_{0}^{\mathscr{T}_f}\mathcal{W}^T(s)\mathcal{T}_{ia}\mathcal{W}(s)ds\big).
\end{aligned}\tag{28}$$

We may deduce from Lemma 1 in [39], that

$$\begin{aligned}
\mathbb{E}\{\mathcal{V}_i(\mathcal{X}(t))\} \le e^{\alpha\mathscr{T}_f}\mu^{N_0}\mu^{\frac{\mathscr{T}_f}{\tau_a}}\big(&\mathbb{E}\{\mathcal{V}_i(\mathcal{X}(0))\}\\
&+\lambda_{\max}(\mathcal{T}_{ia})\beta\big)
\end{aligned}\tag{29}$$

Then, by setting $\widetilde{\mathcal{P}}_{ia} = \mathscr{L}^{-\frac{1}{2}}\mathcal{P}_{ia}\mathscr{L}^{-\frac{1}{2}}$, $\widetilde{\mathcal{Q}}_{lia} = \mathscr{L}^{-\frac{1}{2}}\mathcal{Q}_{lia}\mathscr{L}^{-\frac{1}{2}}$, $\widetilde{\mathcal{R}}_{lia} = \mathscr{L}^{-\frac{1}{2}}\mathcal{R}_{lia}\mathscr{L}^{-\frac{1}{2}}$, $(l = 1, 2)$, it is easy to get that

$$\begin{aligned}
\mathbb{E}\{\mathcal{V}_{\sigma(t)}(\mathcal{X}(t))\} &\ge \mathbb{E}\{\mathcal{X}^T(t)\mathcal{P}_{ia}\mathcal{X}(t)\},\\
&\ge \mathbb{E}\{\mathcal{X}^T(t)\mathscr{L}^{\frac{1}{2}}\widetilde{\mathcal{P}}_{ia}\mathscr{L}^{\frac{1}{2}}\mathcal{X}(t)\},\\
&\ge \min_{i\in\mathbb{N}}\lambda_{\max}(\widetilde{\mathcal{P}}_{ia})\mathbb{E}\{\mathcal{X}^T(t)\mathscr{L}\mathcal{X}(t)\},\\
&= \lambda_1\mathbb{E}\{\mathcal{X}^T(t)\mathscr{L}\mathcal{X}(t)\}.
\end{aligned}\tag{30}$$

From the other hand, we acquire

$$\begin{aligned}
&\mathbb{E}\{\mathcal{V}_{\sigma(0)}(\mathcal{X}(0))\}\\
&\le \mathbb{E}\{\mathcal{X}^T(0)\mathcal{P}_{ia}\mathcal{X}(0)\\
&\quad+\int_{-\overline{\tau}}^{0} e^{\alpha s}\mathcal{X}^T(s)\mathcal{Q}_{1ia}\mathcal{X}(s)ds\\
&\quad+\int_{-\overline{d}}^{0} e^{\alpha s}\mathcal{X}^T(s)\mathcal{Q}_{2ia}\mathcal{X}(s)ds\\
&\quad+\overline{\tau}\int_{-\overline{\tau}}^{0}\int_{\theta}^{0} e^{\alpha s}\dot{\mathcal{X}}^T(s)\mathcal{R}_{1ia}\dot{\mathcal{X}}(s)dsd\theta\\
&\quad+\overline{d}\int_{-\overline{d}}^{0}\int_{\theta}^{0} e^{\alpha s}\dot{\mathcal{X}}^T(s)\mathcal{R}_{2ia}\dot{\mathcal{X}}(s)dsd\theta\}\\
&\le \max_{i\in\mathbb{N}}\big(\lambda_{\min}(\widetilde{\mathcal{P}}_{ia})\big)\mathcal{X}^T(0)\mathscr{L}\mathcal{X}(0)\\
&\quad+\overline{\tau}e^{-\alpha\overline{\tau}}\max_{i\in\mathbb{N}}\big(\lambda_{\min}(\widetilde{\mathcal{Q}}_{1ia})\big)\sup_{-\overline{\tau}<\theta<0}\\
&\quad\times\{\mathcal{X}^T(\theta)\mathscr{L}\mathcal{X}(\theta)\}\\
&\quad+\overline{d}e^{-\alpha\overline{d}}\max_{i\in\mathbb{N}}\big(\lambda_{\min}(\widetilde{\mathcal{Q}}_{2ia})\big)\sup_{-\overline{d}<\theta<0}\\
&\quad\times\{\mathcal{X}^T(\theta)\mathscr{L}\mathcal{X}(\theta)\}\\
&\quad+\frac{\overline{\tau}^2}{2}e^{-\alpha\overline{\tau}}\max_{i\in\mathbb{N}}\big(\lambda_{\min}(\widetilde{\mathcal{R}}_{1ia})\big)\sup_{-\overline{\tau}<\theta<0}\\
&\quad\times\{\dot{\mathcal{X}}^T(\theta)\mathscr{L}\dot{\mathcal{X}}(\theta)\}\\
&\quad+\frac{\overline{d}^2}{2}e^{-\alpha\overline{d}}\max_{i\in\mathbb{N}}\big(\lambda_{\min}(\widetilde{\mathcal{R}}_{2ia})\big)\sup_{-\overline{d}<\theta<0}\\
&\quad\times\{\dot{\mathcal{X}}^T(\theta)\mathscr{L}\dot{\mathcal{X}}(\theta)\}\}\\
&\le \Big(\lambda_2+\overline{\tau}e^{-\alpha\overline{\tau}}\lambda_3+\overline{d}e^{-\alpha\overline{d}}\lambda_4+\frac{\overline{\tau}^2}{2}e^{-\alpha\overline{\tau}}\lambda_5+\frac{\overline{d}^2}{2}e^{-\alpha\overline{d}}\lambda_6\Big)\\
&\quad\sup_{-\overline{\tau}<\theta<0,\,-\overline{d}<\theta<0}\\
&\quad\times\Big\{\mathcal{X}^T(\theta)\mathscr{L}\mathcal{X}(\theta),\,\dot{\mathcal{X}}^T(\theta)\mathscr{L}\dot{\mathcal{X}}(\theta)\Big\}\\
&\le \mathscr{W}_1\mathscr{C}_1
\end{aligned}\tag{31}$$

From (29) - (31) we can get that

$$\begin{aligned}
\mathbb{E}\{\mathcal{X}^T(t)\mathscr{L}\mathcal{X}(t)\} &\le \frac{\mathbb{E}\{\mathcal{V}_{\sigma(t)}(\mathcal{X}(t))\}}{\lambda_1},\\
&\le \frac{e^{\alpha\mathscr{T}_f}\mu^{N_0}\mu^{\frac{\mathscr{T}_f}{\tau_a}}\big(\mathcal{V}_{\sigma(0)}(\mathcal{X}(0))+\lambda_{12}\beta\big)}{\lambda_1},\\
&\le \frac{e^{\alpha\mathscr{T}_f}\mu^{N_0}\mu^{\frac{\mathscr{T}_f}{\tau_a}}\big(\mathscr{W}_1\mathscr{C}_1+\lambda_{12}\beta\big)}{\lambda_1}.
\end{aligned}\tag{32}$$

As a result, if the criterion in (15) holds, it is evident that $\mathbb{E}\{\mathcal{X}^T(t)\mathscr{L}\mathcal{X}(t)\} \le \mathscr{C}_2, \forall t \in [0, \mathscr{T}_f]$. Therefore as consequence, as seen by Definition 2, we have strongly established that the closed-loop NSCPS (11) is FTB in respect of $(\mathscr{C}_1, \mathscr{C}_2, \mathscr{T}_f, \beta, \mathscr{L})$. This concludes the proof.

B. FINITE-TIME MIXED H_∞ AND PASSIVITY-BASED CONTROL DESIGN

In this subsection, we extend the result presented in Theorem 1 with the finite-time mixed H_∞ and passivity approach. A set of necessary criteria is derived for enhancing finite-time mixed H_∞ and passivity performance for the closed-loop NSCPS (11) with unknown gain matrices.

Theorem 2: For given communication channel parameter $0 \leq \overline{\beta} \leq 1$, trigger parameter ς_j, nonnegative real scalars $\overline{\tau}, \overline{d}$, the other parameters $\alpha, \mu, \rho, \mathscr{C}_1, \mathscr{C}_2, \mathscr{T}_f, \beta, \theta, \gamma$, then the NSCPS (11) with AETC sampling technique and cyber-attacks is robustly FTB with respect to $(\mathscr{C}_1, \mathscr{C}_2, \mathscr{T}_f, \beta, \mathscr{L})$ and achieves finite-time mixed H_∞ and passivity performance (12), if there exist symmetric matrices $\mathcal{P}_{ia}, \mathcal{Q}_{1ia}, \mathcal{Q}_{2ia}, \mathcal{R}_{1ia}, \mathcal{R}_{2ia}, \Phi_{1j}, \Phi_{2j}$, appropriate dimensioned matrices $\mathcal{Y}_{ja}, \mathcal{M}_{lia}(l = 1, 2)$ and scalars $\beta_{\mathcal{F}}, \beta_{\mathcal{G}}, \epsilon_1$ such that the following LMIs applicable for all $i, j \in \mathcal{R}$ and $a \in \Gamma$:

$$\breve{\Psi} = \begin{bmatrix} \breve{\Psi}_{\nu_1} & * & * \\ \breve{\Psi}_{\nu_2} & -\wp_1 & * \\ \breve{\Psi}_{\nu_3} & 0 & -\wp_2 \end{bmatrix} < 0 \tag{33}$$

$$\mathcal{P}_{ia} \leq \mu\mathcal{P}_{ja}, \mathcal{Q}_{1ia} \leq \mu\mathcal{Q}_{1ja}, \mathcal{Q}_{2ia} \leq \mu\mathcal{Q}_{2ja},$$
$$\mathcal{R}_{1ia} \leq \mu\mathcal{R}_{1ja}, \mathcal{R}_{2ia} \leq \mu\mathcal{R}_{2ja}, \tag{34}$$

$$\mathscr{W}_1\mathscr{C}_1 + \lambda_{12}\beta < \lambda_1\mathscr{C}_2\mu^{N_0}e^{-\alpha\mathscr{T}_f} \tag{35}$$

$$\begin{bmatrix} \mathcal{R}_{lia} & * \\ \mathcal{M}_{lia} & \mathcal{R}_{lia} \end{bmatrix} > 0, (l = 1, 2) \tag{36}$$

and also any switching signal $\sigma(t)$ with the average dwell time fulfilling

$$\tau_a > \tau_a^* = \frac{\mathscr{T}_f \ln\mu}{\mathscr{F}_{\mathscr{A}}} \tag{37}$$

where

$$\breve{\Psi}_{\nu_1} = \begin{bmatrix} \breve{\Psi}_{1\nu} & * & * \\ \breve{\Psi}_{2\nu} & \breve{\Psi}_{3\nu} & * \\ \breve{\Psi}_{4\nu} & 0 & \breve{\Psi}_{5\nu} \end{bmatrix},$$
$$\breve{\Psi}_{\nu_2} = \begin{bmatrix} \breve{\Psi}_{\nu 21}^T & \breve{\Psi}_{\nu 22}^T & \breve{\Psi}_{\nu 23}^T & \breve{\Psi}_{\nu 24}^T & \breve{\Psi}_{\nu 25}^T & \breve{\Psi}_{\nu 26}^T & \breve{\Psi}_{\nu 27}^T \end{bmatrix}^T,$$
$$\breve{\Psi}_{\nu_3} = \begin{bmatrix} \breve{\Psi}_{\nu 31}^T & \breve{\Psi}_{\nu 32}^T & \breve{\Psi}_{\nu 33}^T & \breve{\Psi}_{\nu 34}^T \end{bmatrix}^T,$$
$$\wp_1 = \mathrm{diag}\{\gamma, 2\nu_1\mathcal{P}_{ia} - \nu_1^2\mathcal{R}_{1ia}, 2\nu_2\mathcal{P}_{ia} - \nu_2^2\mathcal{R}_{2ia}, 2\nu_1\mathcal{P}_{ia} - \nu_1^2\mathcal{R}_{1ia}, 2\nu_2\mathcal{P}_{ia} - \nu_2^2\mathcal{R}_{2ia}, \beta_{\mathcal{F}}, \beta_{\mathcal{G}}\},$$
$$\wp_2 = \mathrm{diag}\{\epsilon_{1i}, \epsilon_{1i}, \epsilon_{1i}, \epsilon_{1i}\},$$
$$\breve{\Psi}_{1\nu} = \begin{bmatrix} \breve{\Psi}_{1\nu 11} & * & * \\ \breve{\Psi}_{1\nu 21} & \breve{\Psi}_{1\nu 22} & * \\ \breve{\Psi}_{1\nu 31} & \breve{\Psi}_{1\nu 32} & \breve{\Psi}_{1\nu 33} \end{bmatrix},$$
$$\breve{\Psi}_{2\nu} = \begin{bmatrix} e^{-\alpha\overline{d}}(\mathcal{R}_{2ia} - \mathcal{M}_{2ia}) & 0 & 0 \\ e^{-\alpha\overline{d}}\mathcal{M}_{2ia} & 0 & 0 \\ 2\mathcal{C}_i^T\mathcal{P}_{ia}^T & 0 & 0 \end{bmatrix},$$
$$\breve{\Psi}_{3\nu} = \begin{bmatrix} \breve{\Psi}_{3\nu 11} & * & * \\ \breve{\Psi}_{3\nu 21} & \breve{\Psi}_{3\nu 22} & * \\ 0 & 0 & -\beta_{\mathcal{F}} \end{bmatrix},$$
$$\breve{\Psi}_{4\nu} = \begin{bmatrix} 2(1-\overline{\beta})(1+\Delta_q)\varphi_a^T\mathcal{Y}_{ja}^T\mathcal{B}_i^T & 0 & 0 \\ 2\overline{\beta}(1+\Delta_q)\varphi_a^T\mathcal{Y}_{ja}^T\mathcal{B}_i^T & 0 & 0 \\ 2\mathcal{D}_i^T\mathcal{P}_{ia}^T - 2(1-\theta)\mathcal{E}_i & 0 & 0 \end{bmatrix},$$
$$\breve{\Psi}_{1\nu 11} = 2\mathcal{P}_{ia}\mathcal{A}_i + \mathcal{Q}_{lia} - e^{-\alpha\overline{\tau}}\mathcal{R}_{1ia} - e^{-\alpha\overline{d}}\mathcal{R}_{2ia} + \alpha\mathcal{P}_{ia},$$
$$\breve{\Psi}_{1\nu 21} = 2\overline{\beta}(1+\Delta_q)\varphi_a^T\mathcal{Y}_{ja}^T\mathcal{B}_i^T + e^{-\alpha\overline{\tau}}(\mathcal{R}_{1ia} - \mathcal{M}_{1ia}),$$
$$\breve{\Psi}_{1\nu 22} = e^{-\alpha\overline{\tau}}(-2\mathcal{R}_{1ia} + \mathcal{M}_{1ia}^T + \mathcal{M}_{1ia}) + \varsigma_j\Phi_{2j},$$
$$\breve{\Psi}_{1\nu 31} = e^{-\alpha\overline{\tau}}\mathcal{M}_{1ia},\ \breve{\Psi}_{3\nu 11} = 2e^{-\alpha\overline{d}}(-\mathcal{R}_{2ia} + \mathcal{M}_{2ia}),$$
$$\breve{\Psi}_{1\nu 33} = -e^{-\alpha\overline{\tau}}(\mathcal{Q}_{1ia} + \mathcal{R}_{1ia}),\ \breve{\Psi}_{1\nu 32} = e^{-\alpha\overline{\tau}}(\mathcal{R}_{1ia} - \mathcal{M}_{1ia}),$$
$$\breve{\Psi}_{3\nu 21} = e^{-\alpha\overline{d}}(\mathcal{R}_{2ia} - \mathcal{M}_{2ia}),\ \breve{\Psi}_{3\nu 22} = -e^{-\alpha\overline{d}}(\mathcal{Q}_{2ia} - \mathcal{R}_{2ia}),$$
$$\breve{\Psi}_{5\nu} = \mathrm{diag}\{-\beta_{\mathcal{G}}, -\Phi_{1j}, -\gamma - 2(1-\theta)\mathcal{H}_i^T\},$$
$$\breve{\Psi}_{\nu 21} = \begin{bmatrix} \sqrt{\theta}\mathcal{E}_i & 0_{7n} & \sqrt{\theta}\mathcal{H}_i \end{bmatrix},$$
$$\breve{\Psi}_{\nu 22} = \overline{\tau}\big[\mathcal{P}_{ia}\mathcal{A}_i\ \overline{\beta}\mathcal{B}_i\mathcal{Y}_{ja}\varphi_a(1+\Delta_q)\ 0_{3n}\ \mathcal{P}_{ia}\mathcal{C}_i\ (1-\overline{\beta})\mathcal{B}_i\mathcal{Y}_{ja}\varphi_a(1+\Delta_q)\ \overline{\beta}\mathcal{B}_i\mathcal{Y}_{ja}\varphi_a(1+\Delta_q)\ \mathcal{P}_{ia}\mathcal{D}_i\big],$$
$$\breve{\Psi}_{\nu 23} = \overline{d}\big[\mathcal{P}_{ia}\mathcal{A}_i\ \overline{\beta}\mathcal{B}_i\mathcal{Y}_{ja}\varphi_a(1+\Delta_q)\ 0_{3n}\ \mathcal{P}_{ia}\mathcal{C}_i\ (1-\overline{\beta})\mathcal{B}_i\mathcal{Y}_{ja}\varphi_a(1+\Delta_q)\ \overline{\beta}\mathcal{B}_i\mathcal{Y}_{ja}\varphi_a(1+\Delta_q)\ \mathcal{P}_{ia}\mathcal{D}_i\big],$$
$$\breve{\Psi}_{\nu 24} = \overline{\tau}\beta_1(1+\Delta_q) \times \big[0\ \mathcal{B}_i\mathcal{Y}_{ja}\varphi_a\ 0_{4n}\ -\mathcal{B}_i\mathcal{Y}_{ja}\varphi_a\ \mathcal{B}_i\mathcal{Y}_{ja}\varphi_a\ 0\big],$$
$$\breve{\Psi}_{\nu 25} = \overline{d}\beta_1(1+\Delta_q) \times \big[0\ \mathcal{B}_i\mathcal{Y}_{ja}\varphi_a\ 0_{4n}\ -\mathcal{B}_i\mathcal{Y}_{ja}\varphi_a\ \mathcal{B}_i\mathcal{Y}_{ja}\varphi_a\ 0\big],$$
$$\breve{\Psi}_{\nu 26} = \begin{bmatrix} \mathscr{F} & 0_{8n} \end{bmatrix},\ \breve{\Psi}_{\nu 27} = \begin{bmatrix} 0 & \mathscr{G} & 0_{7n} \end{bmatrix},$$
$$\breve{\Psi}_{\nu 31} = \begin{bmatrix} 0_{10n} & \overline{\tau}\mathcal{M}_{ia}^T\mathcal{P}_{ia} & 0_{5n} \end{bmatrix},$$
$$\breve{\Psi}_{\nu 33} = \begin{bmatrix} \mathcal{M}_{ia}^T\mathcal{P}_{ia}\ 0_{15n} \end{bmatrix},$$
$$\breve{\Psi}_{\nu 32} = \breve{\Psi}_{\nu 34} = \begin{bmatrix} \epsilon_{1i}\mathcal{N}_{1i}\ 0_{4n}\ \epsilon_{1i}\mathcal{N}_{2i}\ 0\ \epsilon_{1i}\mathcal{N}_{3i}\ 0_{8n} \end{bmatrix},$$
$$\mathscr{W}_1 = \lambda_2 + \overline{\tau}e^{-\alpha\overline{\tau}}\lambda_3 + \overline{d}e^{-\alpha\overline{d}}\lambda_4 + \frac{\overline{\tau}^2}{2}e^{-\alpha\overline{\tau}}\lambda_5 + \frac{\overline{d}^2}{2}e^{-\alpha\overline{d}}\lambda_6,$$
$$\mathscr{F}_{\mathscr{A}} = \ln(\lambda_1\mathscr{C}_2) - \alpha\mathscr{T}_f - N_0\ln\mu - \ln(\mathscr{W}_1\mathscr{C}_1 + \gamma\beta),$$

and other such parameters are zero. Furthermore, the desired controller gain matrices are computed by $\hat{\mathcal{K}}_{ja} = \mathcal{U}\Lambda^{-1}\mathcal{P}_{11ia}^{-1}\Lambda\mathcal{U}^T\mathcal{Y}_{ja}$.

Proof: The NSCPS (11) is FTB, according to Theorem 1. Under zero initial condition, we will demonstrate the finite-time mixed H_∞ and passivity performance of the closed-loop NSCPS (11). Now, employing the same LKF as in Theorem 1, and using the same derivations and equation of (12), it is easy to compute that

$$\begin{aligned} &\mathbb{E}\big\{\dot{\mathcal{V}}_i(\mathcal{X}(t)) - \alpha\mathcal{V}_i(\mathcal{X}(t)) + \gamma^{-1}\theta\mathcal{Z}^T(t)\mathcal{Z}(t) \\ &\quad - 2(1-\theta)\mathcal{Z}^T(t)\mathcal{W}(t) - \gamma\mathcal{W}^T(t)\mathcal{W}(t)\big\} \\ &= \Xi^T(t)\breve{\Psi}\Xi(t), \end{aligned} \tag{38}$$

where $\breve{\Psi}_{9,1} = \mathcal{D}_i^T\mathcal{P}_{ia}^T, \breve{\Psi}_{10,1} = \sqrt{\theta}\mathcal{D}_i, \breve{\Psi}_{10,9} = \sqrt{\theta}\mathcal{E}_i, \breve{\Psi}_{9,9} = -\gamma - 2(1-\theta)\mathcal{H}_i^T, \breve{\Psi}_{10,10} = -\gamma$, and the remaining terms of $\breve{\Psi} = \Psi$ which are described this way from Theorem 1. In addition, with all positive scalars ν_l $(l = 1, 2)$, owing to $(\mathcal{R}_{lia} - \nu_l^{-1}\mathcal{P}_{ia})\mathcal{R}_{lia}^{-1}(\mathcal{R}_{lia} - \nu_l^{-1}\mathcal{P}_{ia}) \geq 0$, one can obtain

$$-\mathcal{P}_{ia}\mathcal{R}_{lia}^{-1}\mathcal{P}_{ia} \leq -2\nu_l\mathcal{P}_{ia} + \nu_l^2\mathcal{R}_{lia}. \tag{39}$$

Replace $-\mathcal{P}_{ia}\mathcal{R}_{lia}^{-1}\mathcal{P}_{ia}$ by $-2\nu_l\mathcal{P}_{ia} + \nu_l^2\mathcal{R}_{lia}$, $\mathcal{P}_{ia}\mathcal{B}_i\mathcal{K}_{ja}$ by $\mathcal{B}_i\mathcal{P}_{1ia}\mathcal{K}_{ja}$ and define $\mathcal{Y}_{ja} = (\mathcal{U}\Lambda^{-1}\mathcal{P}_{11ia}^{-1}\Lambda\mathcal{U}^T)^{-1}\mathcal{K}_{ja}$ in (13). For obtaining the controller gain matrices, we set

$\overline{\mathscr{I}} = \text{diag}\{\mathscr{I}, \cdots, \mathscr{I}\} \in \mathbb{R}^{10\times 10}$. Pre- and post-multiplying (38) by $\text{diag}\{\overline{\mathscr{I}}, \mathcal{P}_{ia}, \mathcal{P}_{ia}, \mathcal{P}_{ia}, \mathcal{P}_{ia}, \mathscr{I}, \mathscr{I}, \mathscr{I}, \mathscr{I}, \mathscr{I}, \mathscr{I}\}$ as well as its transpose, it is simple to acquire the LMI in (33). Hence, from inequality (38) and (39), we may imply that

$$\mathbb{E}\big\{\dot{\mathcal{V}}_i(\mathcal{X}(t)) - \alpha\mathcal{V}_i(\mathcal{X}(t)) + \gamma^{-1}\theta\mathcal{Z}^T(t)\mathcal{Z}(t) - 2(1-\theta)\mathcal{Z}^T(t)\mathcal{W}(t) - \gamma\mathcal{W}^T(t)\mathcal{W}(t)\big\} < 0. \quad (40)$$

It emerges from a simple calculation that

$$\frac{d}{dt}\{V_i(\mathcal{X}(t))e^{-\alpha t}\} < e^{-\alpha t}\Big[-\gamma^{-1}\theta\mathcal{Z}^T(t)\mathcal{Z}(t) + 2(1-\theta)\mathcal{Z}^T(t)\mathcal{W}(t) + \gamma\mathcal{W}^T(t)\mathcal{W}(t)\Big]. \quad (41)$$

Afterward, by integrating the previously mentioned inequality from 0 to $\mathscr{T}_f$ and utilizing (12), it is possible to conclude that the closed-loop NSCPS (11) is FTB and satisfies mixed H_∞ and passivity performance with respect to $(\mathscr{C}_1, \mathscr{C}_2, \mathscr{T}_f, \beta, \mathscr{L})$. This brings the proof of the theorem to a conclusion.

When the proposed controller scheme is applied to the NSCPS (11) and the network is without cyber-attacks, the closed-loop system (11) requires the following structure:

$$\dot{\mathcal{X}}(t) = \hat{\mathcal{A}}_i(t)\mathcal{X}(t) + \mathcal{B}_i\mathcal{K}_{ja}\varphi_a(1+\Delta_q)\big(e_{\hat{\imath}_k}(t) + \mathcal{X}(t-\tau(t))\big) + \hat{\mathcal{C}}_i(t)\mathcal{F}(\mathcal{X}(t)) + \hat{\mathcal{D}}_i(t)\mathcal{W}(t). \quad (42)$$

The proof in Theorem 2 leads to the following corollary.

Corollary 1: For given trigger parameter ς_j, nonnegative real scalar $\overline{\tau}$, the other parameters $\alpha, \mu, \rho, \mathscr{C}_1, \mathscr{C}_2, \mathscr{T}_f, \beta, \theta, \gamma$, then the switched nonlinear NCS (42) with AETC sampling technique is robustly FTB with respect to $(\mathscr{C}_1, \mathscr{C}_2, \mathscr{T}_f, \beta, \mathscr{L})$ and achieves finite-time mixed H_∞ and passivity performance (12), if there exist symmetric matrices $\mathcal{P}_{ia}, \mathcal{Q}_{1ia}, \mathcal{R}_{1ia}, \Phi_{1j}, \Phi_{2j}$, appropriate dimensioned matrices $\mathcal{Y}_{ja}, \mathcal{M}_{1ia}$ and scalars $\beta_{\mathcal{F}}, \epsilon_1$ such that the following LMIs applicable for all $i, j \in \mathcal{R}$ and $a \in \Gamma$:

$$\tilde{\Psi} = \begin{bmatrix} \tilde{\Psi}_{\nu_1} & * & * \\ \tilde{\Psi}_{\nu_2} & -\wp_1 & * \\ \tilde{\Psi}_{\nu_3} & 0 & -\wp_2 \end{bmatrix} < 0 \quad (43)$$

$$\mathcal{P}_{ia} \le \mu\mathcal{P}_{ja}, \mathcal{Q}_{1ia} \le \mu\mathcal{Q}_{1ja}, \mathcal{R}_{1ia} \le \mu\mathcal{R}_{1ja}, \quad (44)$$

$$\mathscr{W}_1\mathscr{C}_1 + \lambda_{12}\beta < \lambda_1\mathscr{C}_2\mu^{N_0}e^{-\alpha\mathscr{T}_f} \quad (45)$$

$$\begin{bmatrix} \mathcal{R}_{1ia} & * \\ \mathcal{M}_{1ia} & \mathcal{R}_{1ia} \end{bmatrix} > 0, \quad (46)$$

and also any switching signal $\sigma(t)$ with the average dwell time fulfilling

$$\tau_a > \tau_a^* = \frac{\mathscr{T}_f \ln\mu}{\mathscr{F}_{\mathscr{A}}} \quad (47)$$

where

$$\tilde{\Psi}_{\nu_1} = \begin{bmatrix} \tilde{\Psi}_{1\nu} & * \\ \tilde{\Psi}_{2\nu} & \tilde{\Psi}_{3\nu} \end{bmatrix},$$

$$\tilde{\Psi}_{1\nu} = \begin{bmatrix} \tilde{\Psi}_{1\nu 11} & * & * \\ \tilde{\Psi}_{1\nu 21} & \tilde{\Psi}_{1\nu 22} & * \\ \tilde{\Psi}_{1\nu 31} & \tilde{\Psi}_{1\nu 32} & \tilde{\Psi}_{1\nu 33} \end{bmatrix},$$

$$\tilde{\Psi}_{\nu_2} = \begin{bmatrix} \tilde{\Psi}_{\nu 21}^T & \tilde{\Psi}_{\nu 22}^T & \tilde{\Psi}_{\nu 23}^T \end{bmatrix}^T,$$

$$\tilde{\Psi}_{\nu_3} = \begin{bmatrix} \tilde{\Psi}_{\nu 31}^T & \tilde{\Psi}_{\nu 32}^T & \tilde{\Psi}_{\nu 33}^T & \tilde{\Psi}_{\nu 34}^T \end{bmatrix}^T,$$

$$\wp_1 = \text{diag}\{\gamma, -2\nu_1\mathcal{P}_{ia} + \nu_1^2\mathcal{R}_{1ia}, \beta_{\mathcal{F}}\},$$

$$\wp_2 = \text{diag}\{\epsilon_{1i}, \epsilon_{1i}, \epsilon_{1i}, \epsilon_{1i}\},$$

$$\tilde{\Psi}_{2\nu} = \begin{bmatrix} \mathcal{C}_i^T\mathcal{P}_{ia}^T & 0 & 0 \\ 2(1+\Delta_q)\varphi_a^T\mathcal{Y}_{ja}^T\mathcal{B}_i^T & 0 & 0 \\ \mathcal{D}_i^T\mathcal{P}_{ia}^T - 2(1-\theta)\mathcal{E}_i & 0 & 0 \end{bmatrix},$$

$$\tilde{\Psi}_{1\nu 11} = 2\mathcal{P}_{ia}\mathcal{A}_i + \alpha\mathcal{P}_{ia} + \mathcal{Q}_{1ia} - e^{-\alpha\overline{\tau}}\mathcal{R}_{1ia},$$

$$\tilde{\Psi}_{1\nu 21} = 2(1+\Delta_q)\varphi_a^T\mathcal{Y}_{ja}^T\mathcal{B}_i^T + e^{-\alpha\overline{\tau}}(\mathcal{R}_{1ia} - \mathcal{M}_{1ia}),$$

$$\tilde{\Psi}_{1\nu 22} = e^{-\alpha\overline{\tau}}(-2\mathcal{R}_{1ia} + \mathcal{M}_{1ia}^T + \mathcal{M}_{1ia}) + \varsigma_j\Phi_{2j},$$

$$\tilde{\Psi}_{1\nu 31} = e^{-\alpha\overline{\tau}}\mathcal{M}_{1ia},\ \tilde{\Psi}_{1\nu 32} = e^{-\alpha\overline{\tau}}(\mathcal{R}_{1ia} - \mathcal{M}_{1ia}),$$

$$\tilde{\Psi}_{1\nu 33} = -e^{-\alpha\overline{\tau}}(\mathcal{Q}_{1ia} + \mathcal{R}_{1ia}),$$

$$\tilde{\Psi}_{\nu_{23}} = \begin{bmatrix} \mathscr{F} & 0_{5n} \end{bmatrix},$$

$$\tilde{\Psi}_{3\nu} = \text{diag}\{-\beta_{\mathcal{F}}, -\Phi_{1j}, -\gamma - 2(1-\theta)\mathcal{H}_i^T\},$$

$$\mathscr{F}_{\mathscr{A}} = \ln(\lambda_1\mathscr{C}_2) - \alpha\mathscr{T}_f - N_0\ln\mu - \ln(\mathscr{W}_1\mathscr{C}_1 + \gamma\beta),$$

$$\tilde{\Psi}_{\nu_{21}} = \begin{bmatrix} \sqrt{\theta}\mathcal{E}_i & 0_{4n} & \sqrt{\theta}\mathcal{H}_i \end{bmatrix},$$

$$\tilde{\Psi}_{\nu_{22}} = \overline{\tau}\big[\mathcal{P}_{ia}\mathcal{A}_i \ \mathcal{B}_i\mathcal{Y}_{ja}\varphi_a(1+\Delta_q)\ 0\ \mathcal{P}_{ia}\mathcal{C}_i\ \mathcal{B}_i\mathcal{Y}_{ja}\varphi_a(1+\Delta_q)\ \mathcal{P}_{ia}\mathcal{D}_i\big],$$

$$\tilde{\Psi}_{\nu_{31}} = \begin{bmatrix} 0_{7n} & \overline{\tau}\mathcal{M}_{ia}^T\mathcal{P}_{ia} & 0 \end{bmatrix},\ \tilde{\Psi}_{\nu_{33}} = \begin{bmatrix} \mathcal{M}_{ia}^T\mathcal{P}_{ia} & 0_{8n} \end{bmatrix},$$

$$\tilde{\Psi}_{\nu_{32}} = \tilde{\Psi}_{\nu_{34}} = \begin{bmatrix} \epsilon_{1i}\mathcal{N}_{1i} & 0_{2n} & \epsilon_{1i}\mathcal{N}_{2i} & 0 & \epsilon_{1i}\mathcal{N}_{3i} & 0_{3n} \end{bmatrix},$$

$$\mathscr{W}_1 = \lambda_2 + \overline{\tau}e^{-\alpha\overline{\tau}}\lambda_3 + \frac{\overline{\tau}^2}{2}e^{-\alpha\overline{\tau}}\lambda_4,$$

and other such parameters are zero. Furthermore, the desired controller gain matrices are computed by $\hat{\mathcal{K}}_{ja} = \mathcal{U}\Lambda^{-1}\mathcal{P}_{11ia}^{-1}\Lambda\mathcal{U}^T\mathcal{Y}_{ja}$.

Remark 3: It is important to highlight that the proposed model incorporates the following significant elements: nonlinear terms, external disturbances, and malicious attacks, all of which contribute to the complexity of network security issues. Specifically, this article focuses on cyberattacks, which aim to manipulate transmission data by completely altering the original information using malicious signal interference. In this context, these attack signals are represented as a nonlinear function denoted as $\mathcal{G}(\mathcal{X}(t))$. Furthermore, it's worth noting that simplifying such nonlinear functions in the derivation of Theorem 1 can be quite challenging due to the presence of AETC. In order to tackle this challenge, the article employs the definition of $\mathcal{G}(\mathcal{X}(t))$ as outlined in Assumption 1 to resolve the nonlinear functions. In light of these considerations, Theorem 1 provides the FTB analysis for a class of NCS subject to cyber-attacks. Furthermore, the design of the Lyapunov-Krasovskii function plays a constructive role in reducing conservatism. A complex Lyapunov-Krasovskii functional with multiple integration terms brings a greater number of decision variables to the

LMIs. Consequently, the computational complexity increases when the number of decision variables increases. So, there should be a trade-off between the integral terms in the construction of the Lyapunov-Krasovskii functional and the LMI constraints. In this paper, we have chosen an appropriate LKF of the form (18) without using any free-weighting matrix technique, which results in less computational burden.

Remark 4: It should be noted that the LMI-based conditions obtained in this work include several tuning parameters, namely, $\overline{\beta}, \overline{\tau}, \overline{d}, \alpha, \mu, \rho, \mathscr{C}_1, \mathscr{C}_2, \mathscr{T}_f, \beta, \theta, \gamma$, Although the solvability of the LMI constraints seems to be easy using any standard numerical software, the selection of the above parameters is quite difficult. This is because these parameters can affect the feasibility of the obtained LMIs. A simple way to select these parameters is to fine-tune them by the trial-and-error method.

IV. NUMERICAL EXAMPLE

Example 1: The helicopter serves a wide range of applications, including military and civilian aviation, agriculture, and various other sectors. The ability for a helicopter to take off and land vertically significantly impacts its dynamic capabilities. Therefore, exploring methods to maintain stable performance during vertical take-off and landing in real-world operations is a subject that merits investigation.

However, in practical operational scenarios, numerous physical systems can experience unpredictable variations in their parameters, resulting in abrupt changes in these parameters or even their overall configurations. The utilization of switched signals plays a crucial role in the examination and design of the VTOLHM. In this example, the VTOLHM will be represented as a switched system, as detailed in references [43], [44], and [45]. Moreover, consider $\mathcal{X}(t) = \left[\mathcal{X}_1^T(t)\ \mathcal{X}_2^T(t)\ \mathcal{X}_3^T(t)\ \mathcal{X}_4^T(t)\right]^T$ represents the state variables, encompassing the following components: horizontal velocity represented by $\mathcal{X}_1(t)$, vertical velocity indicated by $\mathcal{X}_2(t)$, pitch rate denoted by $\mathcal{X}_3(t)$, and pitch angle represented by $\mathcal{X}_4(t)$. The behavior of $\sigma(t)$ is modeled as switching signal with the airspeeds of 135 ($\sigma(t) = 1$), 60 ($\sigma(t) = 2$), and 170 ($\sigma(t) = 3$) knots. From the above airspeeds, we can see that the vertical take-off and landing helicopter runs at different speeds. The transformation between different speeds obeys switched signals. The relevant matrix values are borrowed from [43], [44], and [45] and are given as follows ($i = 1, 2, 3$) :

$$\mathcal{A}_i = \begin{bmatrix} -0.0366 & 0.0271 & 0.0188 & -0.4555 \\ 0.0482 & -1.0100 & 0.0024 & -4.0208 \\ 0.1002 & a_{32i} & -0.7070 & a_{34i} \\ 0 & 0 & 1 & 0 \end{bmatrix},$$

$$\mathcal{B}_i = \begin{bmatrix} 0.4422 & 0.1761 \\ b_{21i} & -7.5922 \\ -5.5200 & 4.4900 \\ 0 & 0 \end{bmatrix}.$$

where, $a_{321} = 0.3681, a_{322} = 0.00664, a_{323} = 0.5047, a_{341} = 1.4200, a_{342} = 0.1198, a_{343} = 2.5460, b_{211} = 3.5446, b_{212} = 0.9775$ and $b_{213} = 5.1120$. Further, we choose the other matrices of NSCPS (11) as follows:

$$\mathcal{C}_1 = \mathcal{C}_2 = \mathcal{C}_3 = \begin{bmatrix} 0.01 & 0.1 & 0.1 & 0 \\ 0.1 & 0.1 & 0 & 0.1 \\ 0.2 & 0.3 & 0.4 & 0.1 \\ 0.2 & 0.4 & 0.1 & 0.1 \end{bmatrix},$$

$$\mathcal{D}_1 = \mathcal{D}_2 = \mathcal{D}_3 = \begin{bmatrix} 0.2 & 0.1 & 0.1 & 0.2 \end{bmatrix}^T,$$

$$\mathcal{E}_1 = \mathcal{E}_2 = \mathcal{E}_3 = \begin{bmatrix} 0.2 & 0.1 & 0.0 & 0.1 \end{bmatrix},$$

$$\mathcal{M}_{11} = \mathcal{M}_{12} = \mathcal{M}_{13} = \text{diag}\{0.1, 0.3, 0.1, 0.2\}$$

$$\mathcal{N}_{11} = \mathcal{N}_{12} = \mathcal{N}_{13} = \text{diag}\{0.1, 0.3, 0.1, 0.2\},$$

$$\mathcal{N}_{21} = \mathcal{N}_{22} = \mathcal{N}_{23} = \text{diag}\{0.1, 0.2, 0.3, 0.2\},$$

$$N_{31} = \mathcal{N}_{32} = \mathcal{N}_{33} = \begin{bmatrix} 0.1 & 0.3 & 0 & 0.2 \end{bmatrix}^T,$$

$$\mathcal{H}_1 = \mathcal{H}_2 = \mathcal{H}_3 = 0.1,\ \mathcal{F}(\mathcal{X}(t)) = \begin{bmatrix} \tanh(-0.1\mathcal{X}_1(t)) \\ \tanh(0.1\mathcal{X}_2(t)) \\ \tanh(-0.1\mathcal{X}_3(t)) \\ \tanh(0.1\mathcal{X}_4(t)) \end{bmatrix}.$$

For the purpose of simulation, the exogenous disturbance are taken as $\mathcal{W}(t) = 0.2\exp(-0.01t)r$, where $r = a + (b - a)\text{rand}n, a = -0.5, b = 0.5$. Furthermore, it is assumed that the cyber-attack function is $\mathcal{G}(\mathcal{X}(t)) = [\tanh(-0.5\mathcal{X}_1(t)), \tanh(0.5\mathcal{X}_2(t)), \tanh(-0.5\mathcal{X}_3(t)), \tanh(0.5\mathcal{X}_4(t))]^T$. We use $\rho(t) \in \{1, 2\}$ throughout each transmission to minimize the measurement size and

$$\varphi_{\rho(t)} \in \left\{ \begin{bmatrix} 1 & 0 & 0 & 0 \\ 0 & 1 & 0 & 0 \\ 0 & 0 & 0 & 0 \\ 0 & 0 & 0 & 0 \end{bmatrix}, \begin{bmatrix} 0 & 0 & 0 & 0 \\ 0 & 0 & 0 & 0 \\ 0 & 0 & 1 & 0 \\ 0 & 0 & 0 & 1 \end{bmatrix} \right\}.$$

Furthermore, we explore two cases to validate the applicability of the suggested control design method. Case 1 considers both the AETC scheme and cyber-attacks for NSCPS (11), while Case 2 considers only the AETC strategy for switched nonlinear NCS (42).

Case 1: Let the cyber-attack and the event based parameters are chosen as $\overline{\beta} = 0.6$, and $\varsigma_j = 0.5$. Furthermore, its remaining parameters are described as follows: $\gamma = 0.9$, $\theta = 0.7$, $\mu = 1.05$, $\alpha = 0.005$, $\rho = 0.6$, $\overline{\tau} = 0.01$, $\overline{d} = 0.01$, $\mathscr{C}_1 = 0.7$, $\mathscr{C}_2 = 1.7657$, $\mathscr{T}_f = 50$ and $\beta = 0.7$. Then, the LMI constraints obtained in (33) are solved by employing MATLAB LMI toolbox and the feasibility can be obtained with aforementioned parameter values. Based on which, the feedback gain matrices can be projected by

$$\mathcal{K}_{11} = \begin{bmatrix} 0.0217 & 0.0174 & 0 & 0 \\ 0.0127 & 0.0083 & 0 & 0 \end{bmatrix},$$

$$\mathcal{K}_{21} = \begin{bmatrix} 0.0053 & -0.0011 & 0 & 0 \\ -0.0012 & -0.0012 & 0 & 0 \end{bmatrix},$$

$$\mathcal{K}_{31} = \begin{bmatrix} 0.0020 & 0.0025 & 0 & 0 \\ 0.0015 & 0.0006 & 0 & 0 \end{bmatrix},$$

$$\mathcal{K}_{12} = \begin{bmatrix} 0 & 0 & 0.0137 & 0.0095 \\ 0 & 0 & 0.0090 & -0.0035 \end{bmatrix},$$

TABLE 1. $\overline{\tau}$ and $\overline{d}$ were calculated for various γ values.

γ	0.1	0.3	0.5	0.7	0.9
$\overline{\tau} = \overline{d}$	0.303	0.306	0.307	0.308	0.309

TABLE 2. $\overline{\tau}$ and $\overline{d}$ were calculated for various α values.

α	0.005	0.01	0.05	0.07	0.09
$\overline{\tau} = \overline{d}$	0.309	0.308	0.307	0.306	0.305

TABLE 3. Calculated $\overline{\tau} = \overline{d}$ for different performances.

Performances	Passivity ($\theta = 0$)	Mixed H_∞ and Passivity ($\theta = 0.7$)	H_∞ ($\theta = 1$)
$\overline{\tau} = \overline{d}$	0.307	0.309	0.308

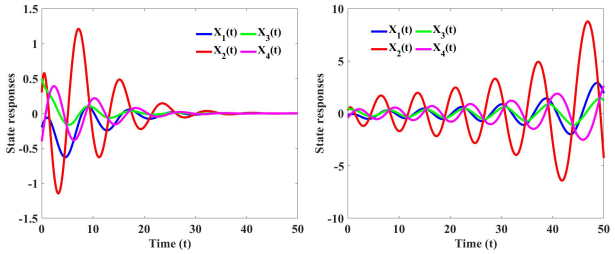

(a) With control (b) Without control

FIGURE 2. State responses of NSCPS (11).

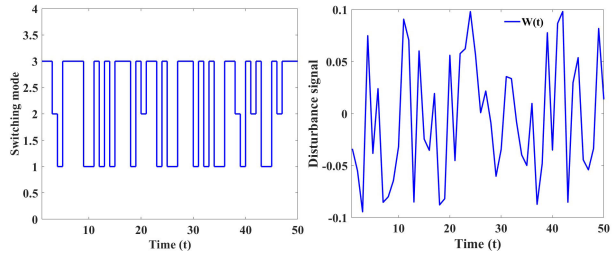

(a) (b)

FIGURE 3. Simulation results of switching and disturbances input signals for NSCPS (11).

$$\mathcal{K}_{22} = \begin{bmatrix} 0 & 0 & -0.0176 & -0.0078 \\ 0 & 0 & -0.0026 & -0.0103 \end{bmatrix},$$
$$\mathcal{K}_{32} = \begin{bmatrix} 0 & 0 & -0.0084 & 0.0197 \\ 0 & 0 & -0.0060 & 0.0077 \end{bmatrix}.$$

For simulation purposes, the initial state is considered to be $\mathcal{X}(0) = \begin{bmatrix} -0.2 & 0.3 & 0.5 & -0.4 \end{bmatrix}^T$ and the average dwell time τ_a^* on the switching signal $\sigma(t)$ can be determined as $\tau_a^* = 6.0096$. As a result, the simulated results are shown in Figs. 2-7 depending on the aforesaid controller gain matrices. To summarize, the state trajectories of NSCPS (11) with and without controller, which are seen in Fig. 2(a) and 2(b). Then, the corresponding switching signal $\sigma(t)$ and the disturbances input signal $\mathcal{W}(t)$ are depicted in Fig. 3(a) and 3(b). Further, Fig. 4(a) and 4(c) depicts the time evolution of $\mathbb{E}\{\mathcal{X}^T(t)\mathcal{L}\mathcal{X}(t)\}$, where it clearly showcases that the state doesn't surpass the value $\mathscr{C}_2$. The

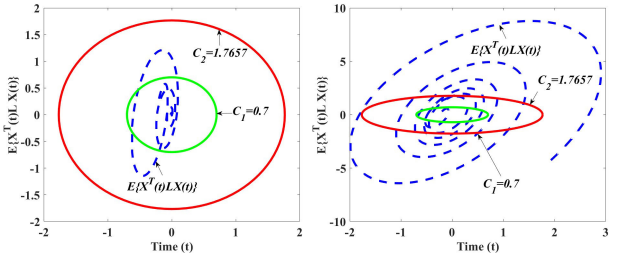

(a) With control (b) Without control

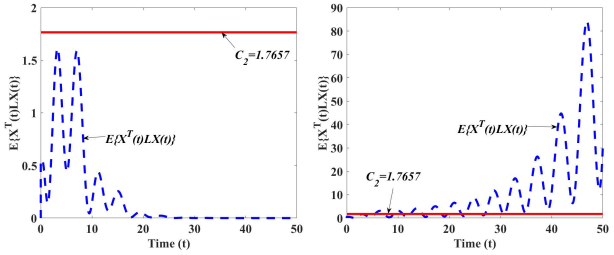

(c) With control (d) Without control

FIGURE 4. Evaluation $\mathbb{E}\{\mathcal{X}^T(t)\mathcal{L}\mathcal{X}(t)\}$ of NSCPS (11).

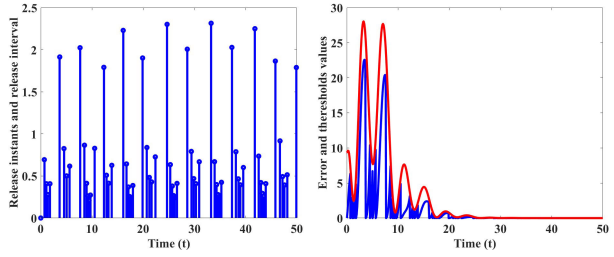

(a) (b)

FIGURE 5. Responses of release instants and release interval, error and theresholds for NSCPS (11).

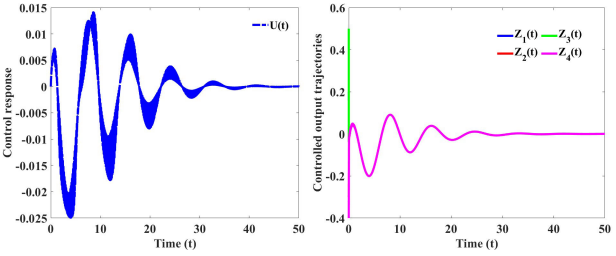

(a) (b)

FIGURE 6. Controlled and output trajectories for NSCPS (11).

time evolution of $\mathbb{E}\{\mathcal{X}^T(t)\mathcal{L}\mathcal{X}(t)\}$ without controller is displayed in Fig. 4(b) and 4(d). As a result, it is clear that the suggested control can maintain the stability of the considered system though in the existence of cyber-attacks. The curves of an ETC release instants and intervals, error and theresholds values are displayed in Fig. 5(a) and 5(b), respectively. In Fig. 6(a) and 6(b), the controlled and output trajectories are given. Furthermore, the cyber-attack function

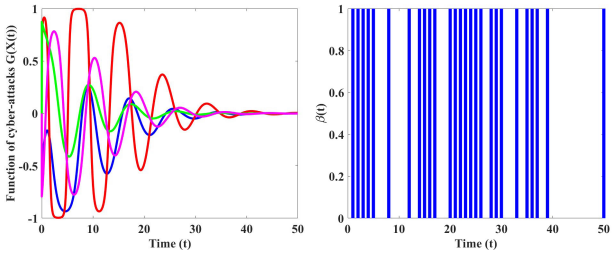

(a) (b)

FIGURE 7. Response of cyber-attack function $\mathcal{G}(\mathcal{X}(\cdot))$ and stochastic variable $\beta(t)$.

TABLE 4. $\overline{\tau}$ was calculated for various for various γ values.

γ	0.1	0.2	0.4	0.9
$\overline{\tau}$	0.362	0.363	0.364	0.365

TABLE 5. $\overline{\tau}$ was calculated for various for various α values.

α	0.005	0.01	0.05	0.07	0.09
$\overline{\tau}$	0.365	0.364	0.363	0.361	0.359

$\mathcal{G}(\mathcal{X}(\cdot))$ and Bernoulli distributed stochastic variable $\beta(t)$ are presented in Fig. 7(a) and 7(b). The calculated upperbound of maximum time-delays $\overline{\tau}$ and $\overline{d}$ for various γ values are disclosed in TABLE 1 and also for various α values are indexed in TABLE 2. Furthermore, $\overline{\tau}$ and $\overline{d}$ values for several instances, namely, passivity, mixed H_∞ & passivity and H_∞ performance are presented in TABLE 3.

As can be seen from the simulation results, the NSCPS in (11) even in the presence of AETC scheme and quantization effect is robustly FTB with respect to $(0.7, 1.7657, 50, 0.7, I)$ and has a reasonable finite-time mixed H_∞ and passivity performance, demonstrating the suggested controller design's adaptability under cyber-attacks.

Case 2: Here, we set $\overline{\beta} = 0$, that is the NCS (42) works normally without cyber-attacks. Hence, with the same parameter values carried out in the previous case, the desired controller gains without cyber-attack are established by

$$\mathcal{K}_{11} = \begin{bmatrix} 0.0393 & 0.0413 & 0 & 0 \\ 0.0106 & 0.0089 & 0 & 0 \end{bmatrix},$$
$$\mathcal{K}_{21} = \begin{bmatrix} 0.0034 & -0.0043 & 0 & 0 \\ -0.0015 & -0.0076 & 0 & 0 \end{bmatrix},$$
$$\mathcal{K}_{31} = \begin{bmatrix} 0.0151 & 0.0112 & 0 & 0 \\ 0.0088 & 0.0020 & 0 & 0 \end{bmatrix},$$
$$\mathcal{K}_{12} = \begin{bmatrix} 0 & 0 & 0.0114 & 0.0396 \\ 0 & 0 & 0.0031 & -0.0148 \end{bmatrix},$$
$$\mathcal{K}_{22} = \begin{bmatrix} 0 & 0 & -0.0676 & -0.0225 \\ 0 & 0 & -0.0112 & -0.0237 \end{bmatrix},$$
$$\mathcal{K}_{32} = \begin{bmatrix} 0 & 0 & -0.0556 & 0.0623 \\ 0 & 0 & -0.0402 & 0.0260 \end{bmatrix}.$$

Here, the state responses for NCS (42) in the presence and absence of controller are displayed 8(a) and 8(b), respectively. Moreover, the time history $\mathbb{E}\{\mathcal{X}^T(t)\mathscr{L}\mathcal{X}(t)\}$

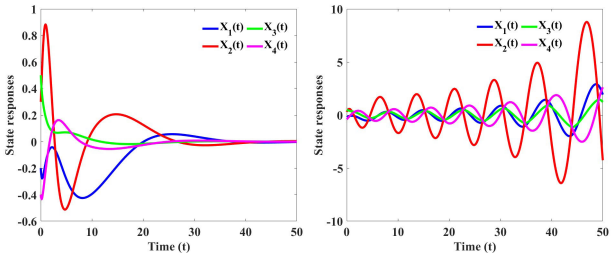

(a) With control (b) Without control

FIGURE 8. State responses of NCS (42).

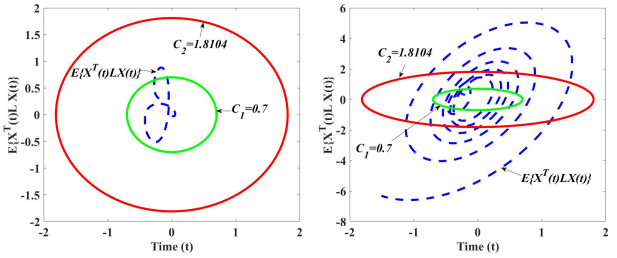

(a) With control (b) Without control

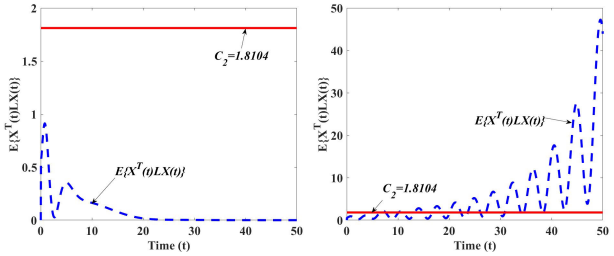

(c) With control (d) Without control

FIGURE 9. Evaluation $\mathbb{E}\{\mathcal{X}^T(t)\mathscr{L}\mathcal{X}(t)\}$ of NCS (42).

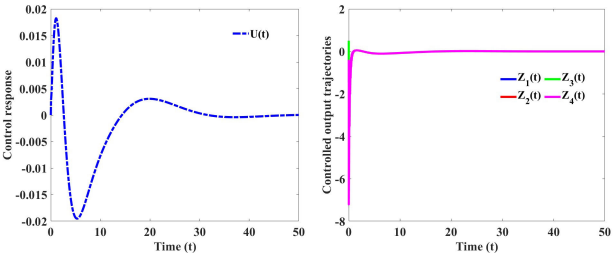

(a) (b)

FIGURE 10. Controlled and output trajectories for NCS (42).

of closed-loop NCS (42) is depicted in Fig. 9(a) and 9(c). It can be viewed from Fig. 9(a) and 9(c) that the desired system (42) without cyber-attack is FTB and does not exceeds the bound $\mathscr{C}_2 = 1.8104$. Furthermore, the time evolution of $\mathbb{E}\{\mathcal{X}^T(t)\mathscr{L}\mathcal{X}(t)\}$, without controller is disclosed in Fig. 9(b) and 9(d). Moreover, the controlled and output trajectories for NCS (42) are plotted in Figs. 10(a) and 10(b), respectively. Further, the release instants and release interval, error and theresholds for NCS (42) are presented in

TABLE 6. Calculated $\overline{\tau}$ for different performances.

Performances	Passivity ($\theta = 0$)	Mixed H_∞ and Passivity ($\theta = 0.7$)	H_∞ ($\theta = 1$)
$\overline{\tau}$	0.363	0.365	0.364

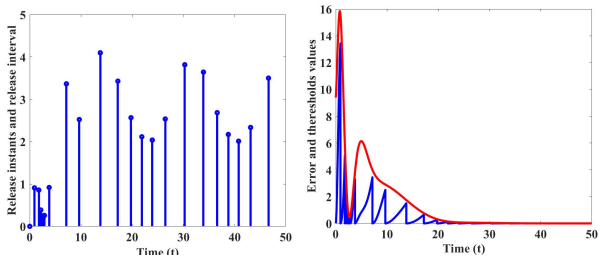

(a) (b)

FIGURE 11. Responses of release instants and release interval, error and theresholds for NCS (42).

Fig. 11(a) and 11(b). Additionally, the calculated time delay $\overline{\tau}$ for various γ and α is provided in TABLES 4 and 5, respectively. Finally, the calculated $\overline{\tau}$ for three different performances are provided in TABLE 6. Thus, it is verified that based AETC mechanism for NCS (42) is FTB with respect to $(0.7, 1.8104, 50, 0.7, I)$.

The simulation results indicate that the unforced NSCPS under investigation are unstable. However, the suggested state feedback control law stabilizes the NSCPS. According to Figs. 2, 4, 8 and 9, the suggested controller effectively stabilizes the NSCPS in both circumstances. Furthermore, as compared to Fig. 2(a), the state trajectories in Fig. 8(a) converge smoothly and quickly to an equilibrium point. Furthermore, TABLES 1-3 clearly show that the time delays for various values of γ, α and the difference performances are better than the values in TABLES 4-6 respectively, implying that the absence of a cyber-attack in the system has less conservative and better performance. As an outcome, it can be claimed that the suggested control mechanism is more realistic since it is more generic and can handle quantization, uncertainty, and cyber-attacks.

V. CONCLUSION

An AETC problem for a category of NSCPS in the presence of energy limitations and quantization across a finite-time period is highlighted in this study. An AETC mechanism and the measurement size reduction techniques are combined in a unified framework to preserve limited power in communication networks. Meanwhile, cyber-attacks that occur at random and attempt to degrade network reliability are represented as a nonlinear function. Nevertheless, in the proposed controller, the external disturbances are compensated by incorporating mixed H_∞ and passivity conditions. A novel collection of adequate requirements in the construction of LMIs ensures the FTB of closed-loop NSCPS with mixed H_∞ and passivity performance with the help of proper LKF. With the use of LMIs, the appropriate controller gain matrices are achieved. Eventually, a VTOLHM example is offered to highlight the significance of the suggested control strategy.

REFERENCES

[1] S.-H. Yang and J.-L. Wu, "Synthesis of fault-tolerant static output feedback controllers for networked control systems," *J. Chin. Inst. Eng.*, vol. 39, no. 5, pp. 600–605, Jul. 2016.

[2] S. Yang and J. Wu, "Mixed event/time-triggered static output feedback L_2-gain control for networked control systems," *Asian J. Control*, vol. 19, no. 1, pp. 1–10, Jan. 2017.

[3] L. Li, J. Fu, Y. Zhang, T. Chai, L. Song, and P. Albertos, "Output regulation for networked switched systems with alternate event-triggered control under transmission delays and packet losses," *Automatica*, vol. 131, Sep. 2021, Art. no. 109716.

[4] S. Shi, Z. Fei, H. R. Karimi, and H.-K. Lam, "Event-triggered control for switched T–S fuzzy systems with general asynchronism," *IEEE Trans. Fuzzy Syst.*, vol. 30, no. 1, pp. 27–38, Jan. 2022.

[5] J. Wu, C. Peng, J. Zhang, M. Yang, and B.-L. Zhang, "Guaranteed cost control of hybrid-triggered networked systems with stochastic cyber-attacks," *ISA Trans.*, vol. 104, pp. 84–92, Sep. 2020.

[6] A. W. A. Saif, "Control for uncertain nonlinear networked control systems with random packet losses," *IEEE Access*, vol. 7, pp. 26179–26191, 2019.

[7] J. Liu, E. Tian, X. Xie, and H. Lin, "Distributed event-triggered control for networked control systems with stochastic cyber-attacks," *J. Franklin Inst.*, vol. 356, no. 17, pp. 10260–10276, Nov. 2019.

[8] T.-F. Li, J. Fu, F. Deng, and T. Chai, "Stabilization of switched linear neutral systems: An event-triggered sampling control scheme," *IEEE Trans. Autom. Control*, vol. 63, no. 10, pp. 3537–3544, Oct. 2018.

[9] H. Ren, G. Zong, and T. Li, "Event-triggered finite-time control for networked switched linear systems with asynchronous switching," *IEEE Trans. Syst., Man, Cybern. Syst.*, vol. 48, no. 11, pp. 1874–1884, Nov. 2018.

[10] J. Wu, "Singular L_2-gain control for switched nonlinear control systems under arbitrary switching," *Int. J. Robust Nonlinear Control*, vol. 30, no. 10, pp. 4149–4163, Jul. 2020.

[11] L. Zhang, S. Wang, H. R. Karimi, and A. Jasra, "Robust finite-time control of switched linear systems and application to a class of servomechanism systems," *IEEE/ASME Trans. Mechatronics*, vol. 20, no. 5, pp. 2476–2485, Oct. 2015.

[12] L. Zhang, S. Zhuang, and R. D. Braatz, "Switched model predictive control of switched linear systems: Feasibility, stability and robustness," *Automatica*, vol. 67, pp. 8–21, May 2016.

[13] G. Zong, H. Ren, and H. R. Karimi, "Event-triggered communication and annular finite-time $H\infty$ filtering for networked switched systems," *IEEE Trans. Cybern.*, vol. 51, no. 1, pp. 309–317, Jan. 2021.

[14] D. Zhang, Z. Xu, H. R. Karimi, and Q.-G. Wang, "Distributed filtering for switched linear systems with sensor networks in presence of packet dropouts and quantization," *IEEE Trans. Circuits Syst. I, Reg. Papers*, vol. 64, no. 10, pp. 2783–2796, Oct. 2017.

[15] J. Liu, N. Zhang, Y. Li, X. Xie, E. Tian, and J. Cao, "Learning-based event-triggered tracking control for nonlinear networked control systems with unmatched disturbance," *IEEE Trans. Syst., Man, Cybern. Syst.*, vol. 53, no. 5, pp. 3230–3240, May 2023.

[16] E. Tian and C. Peng, "Memory-based event-triggering H_∞ load frequency control for power systems under deception attacks," *IEEE Trans. Cybern.*, vol. 50, no. 11, pp. 4610–4618, Nov. 2020.

[17] L. Zha, R. Liao, J. Liu, X. Xie, E. Tian, and J. Cao, "Dynamic event-triggered output feedback control for networked systems subject to multiple cyber attacks," *IEEE Trans. Cybern.*, vol. 52, no. 12, pp. 13800–13808, Dec. 2022.

[18] Z. Fei, C. Guan, and X. Zhao, "Event-triggered dynamic output feedback control for switched systems with frequent asynchronism," *IEEE Trans. Autom. Control*, vol. 65, no. 7, pp. 3120–3127, Jul. 2020.

[19] J.-Y. Jhang, J.-L. Wu, and C.-F. Yung, "Design of event-triggered state-constrained stabilizing controllers for nonlinear control systems," *IEEE Access*, vol. 10, pp. 3659–3667, 2022.

[20] X. Zhao, H. Chen, Z. Zhang, S. Dong, S. Zhong, and Z. You, "Dynamic event-triggered control on nonlinear asynchronous switched system with mixed time-varying delays," *J. Frank. Inst.*, vol. 359, no. 1, pp. 520–555, 2022.

[21] Y. Qi, Y. Liu, and B. Niu, "Event-triggered H_∞ filtering for networked switched systems with packet disorders," *IEEE Trans. Syst., Man, Cybern. Syst.*, vol. 51, no. 5, pp. 2847–2859, May 2021.
[22] X. Xiao, J. H. Park, and L. Zhou, "Event-triggered control of discrete-time switched linear systems with packet losses," *Appl. Math. Comput.*, vol. 333, pp. 344–352, Sep. 2018.
[23] S. Shi, Z. Fei, Z. Shi, and S. Ren, "Stability and stabilization for discrete-time switched systems with asynchronism," *Appl. Math. Comput.*, vol. 338, pp. 520–536, Dec. 2018.
[24] H. Shen, M. Chen, Z.-G. Wu, J. Cao, and J. H. Park, "Reliable event-triggered asynchronous extended passive control for semi-Markov jump fuzzy systems and its application," *IEEE Trans. Fuzzy Syst.*, vol. 28, no. 8, pp. 1708–1722, Aug. 2020.
[25] J. Liu, Y. Gu, J. Cao, and S. Fei, "Distributed event-triggered H_∞ filtering over sensor networks with sensor saturations and cyber-attacks," *ISA Trans.*, vol. 81, pp. 63–75, Oct. 2018.
[26] L. Zha, E. Tian, X. Xie, Z. Gu, and J. Cao, "Decentralized event-triggered H_∞ control for neural networks subject to cyber-attacks," *Inf. Sci.*, vols. 457–458, pp. 141–155, Aug. 2018.
[27] M. Segovia-Ferreira, J. Rubio-Hernan, R. Cavalli, and J. Garcia-Alfaro, "Switched-based resilient control of cyber-physical systems," *IEEE Access*, vol. 8, pp. 212194–212208, 2020.
[28] S. Liu, Y. Liu, S. Li, and B. Xu, "H_∞ control for time-varying cyber-physical system under randomly occurring hybrid attacks: The output feedback case," *IEEE Access*, vol. 8, pp. 60780–60789, 2020.
[29] E. Tian, H. Chen, C. Wang, and L. Wang, "Security-ensured state of charge estimation of lithium-ion batteries subject to malicious attacks," *IEEE Trans. Smart Grid*, vol. 14, no. 3, pp. 2250–2261, May 2023.
[30] Z. Cao, Y. Niu, and J. Song, "Finite-time sliding-mode control of Markovian jump cyber-physical systems against randomly occurring injection attacks," *IEEE Trans. Autom. Control*, vol. 65, no. 3, pp. 1264–1271, Mar. 2020.
[31] J. Liu, E. Gong, L. Zha, X. Xie, and E. Tian, "Outlier-resistant recursive security filtering for multirate networked systems under fading measurements and round-robin protocol," *IEEE Trans. Control Netw. Syst.*, early access, Mar. 13, 2023, doi: 10.1109/TCNS.2023.3256299.
[32] J. Liu, Z.-G. Wu, D. Yue, and J. H. Park, "Stabilization of networked control systems with hybrid-driven mechanism and probabilistic cyber attacks," *IEEE Trans. Syst., Man, Cybern. Syst.*, vol. 51, no. 2, pp. 943–953, Feb. 2021.
[33] D. Zhang, D. Srinivasan, L. Yu, W.-A. Zhang, and K. Xing, "Distributed non-fragile filtering in sensor networks with energy constraints," *Inf. Sci.*, vols. 370–371, pp. 695–707, Nov. 2016.
[34] D. Zhang, Z. Xu, D. Srinivasan, and L. Yu, "Leader–follower consensus of multiagent systems with energy constraints: A Markovian system approach," *IEEE Trans. Syst., Man, Cybern. Syst.*, vol. 47, no. 7, pp. 1727–1736, Jul. 2017.
[35] J. Song, Y. Niu, and Y. Zou, "Finite-time stabilization via sliding mode control," *IEEE Trans. Autom. Control*, vol. 62, no. 3, pp. 1478–1483, Mar. 2017.
[36] Z. Yan, W. Zhang, and G. Zhang, "Finite-time stability and stabilization of Itô stochastic systems with Markovian switching: Mode-dependent parameter approach," *IEEE Trans. Autom. Control*, vol. 60, no. 9, pp. 2428–2433, Sep. 2015.
[37] H. Pang and S. Liu, "Robust finite time passivity and stabilization of uncertain switched nonlinear system," *IEEE Access*, vol. 9, pp. 36173–36180, Mar. 2021.
[38] S. Jin, A. Yan, Y. Pang, B. Zhou, and S. Sun, "Robust finite-time H_∞ filtering for uncertain switched systems with state constraints and multiple time delays," *IEEE Access*, vol. 8, pp. 145457–145468, 2020.
[39] H. Liu, Y. Shen, and X. Zhao, "Delay-dependent observer-based H_∞ finite-time control for switched systems with time-varying delay," *Nonlinear Anal., Hybrid Syst.*, vol. 6, no. 3, pp. 885–898, Aug. 2012.
[40] Z.-L. Zhao, Z.-P. Jiang, T. Liu, and T. Chai, "Global finite-time output-feedback stabilization of nonlinear systems under relaxed conditions," *IEEE Trans. Autom. Control*, vol. 66, no. 9, pp. 4259–4266, Sep. 2021.
[41] C.-H. Zhang and G.-H. Yang, "Event-triggered global finite-time control for a class of uncertain nonlinear systems," *IEEE Trans. Autom. Control*, vol. 65, no. 3, pp. 1340–1347, Mar. 2020.
[42] Y. Qi, P. Zeng, and W. Bao, "Event-triggered and self-triggered H_∞ control of uncertain switched linear systems," *IEEE Trans. Syst., Man, Cybern. Syst.*, vol. 50, no. 4, pp. 1442–1454, Apr. 2020.
[43] D. P. De Farias, J. C. Geromel, J. B. R. Do Val, and O. L. V. Costa, "Output feedback control of Markov jump linear systems in continuous-time," *IEEE Trans. Autom. Control*, vol. 45, no. 5, pp. 944–949, May 2000.
[44] W. Qi, J. H. Park, G. Zong, J. Cao, and J. Cheng, "Anti-windup design for saturated semi-Markovian switching systems with stochastic disturbance," *IEEE Trans. Circuits Syst. II, Exp. Briefs*, vol. 66, no. 7, pp. 1187–1191, Jul. 2019.
[45] W. Qi, Y. Hou, G. Zong, and C. K. Ahn, "Finite-time event-triggered control for semi-Markovian switching cyber-physical systems with FDI attacks and applications," *IEEE Trans. Circuits Syst. I, Reg. Papers*, vol. 68, no. 6, pp. 2665–2674, Jun. 2021.

ARUMUGAM ARUNKUMAR received the B.Sc., M.Sc., and M.Phil. degrees in mathematics from Bharathiar University, Coimbatore, India, in 2006, 2008, and 2009, respectively, and the Ph.D. degree in mathematics from Anna University, Chennai, India, in 2013. From 2014 to 2016, he was an Assistant Professor with the Department of Mathematics, Karpagam Academy of Higher Education, Coimbatore, India. From 2017 to 2021, he was a Postdoctoral Research Fellow with the Department of Mathematics, Yangzhou University, China. He is currently a Postdoctoral Research Fellow with the Department of Electrical Engineering, National Taiwan Ocean University, Keelung, Taiwan. To the credit, he has published more than 35 research papers in Science Citation Index journals. His current research interests include nonlinear networked systems, robust control for uncertain systems, state-constrained control, and delay differential systems.

JENQ-LANG WU (Member, IEEE) received the B.S. and Ph.D. degrees in electrical engineering from the National Taiwan University of Science and Technology, Taipei, Taiwan, in 1991 and 1996, respectively.

He is currently a Professor with the Department of Electrical Engineering, National Taiwan Ocean University, Keelung, Taiwan. His current research interests include nonlinear control systems, state-constrained control, structural-constrained controller design, and multiobjective control.

Dr. Wu was a recipient of the 2009 Ta-You Wu Memorial Award of the National Science Council of Taiwan.